
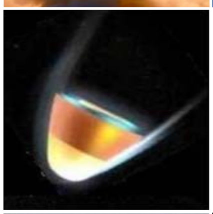
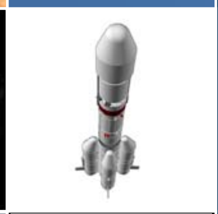
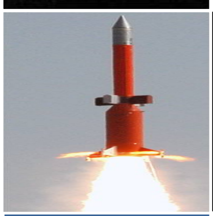
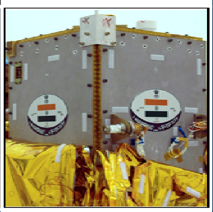
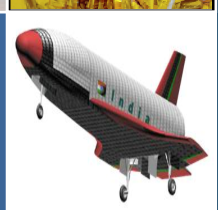

OTAP REFERENCE MANUAL: VERSION 1.0

AERODYNAMIC HEATING & THERMAL ANALYSIS DIVISION

AERODYNAMICS & AEROTHERMAL GROUP

AERONAUTICS ENTITY

VIKRAM SARABHAI SPACE CENTRE

THIRUVANANTHAPURAM

September 2010

Issue No.: 1

Copy No.:

Date of Issue: 14 09 2010

Doc No: **VSSC/AHTD/SP/001/2010**

Security Classification: Unclassified

Control Status: **Controlled**

OTAP REFERENCE MANUAL: VERSION 1.0

	Name	Signature	Date
Compiled By	Ram Prabhu. M Anoop. P Rony C. Varghese Dr. T. V. Radhakrishnan ***(Members, Task team)***		14 09 2010
Reviewed By	Sundar. B ***Convenor, Task team***		14 09 2010
Approved By	R. Swaminathan ***Chairman, Task team***		14 09 2010

AERODYNAMIC HEATING & THERMAL ANALYSIS DIVISION
AERODYNAMICS & AEROTHERMAL GROUP
AERONAUTICS ENTITY
VIKRAM SARABHAI SPACE CENTRE
THIRUVANANTHAPURAM – 695022

Document Control Sheet

01	Security Classification: Unclassified			02	Distribution: Restricted	
03	Report Status:	04	Series:	05	Report Type: Technical memorandum	
06	Report No.: **VSSC/AHTD/SP/01/2010**	07	Part No.: Or Vol. No.:	08	Contract No.:	
09	**Title & Subtitle:** OTAP REFERENCE MANUAL: VERSION 1.0					
10	Collation: Pages: 70 Figures: 12			11	Project No.:	
12	Personal author(s): Ram Prabhu M, Anoop P, Rony C Varghese & Dr T V Radhakrishnan					
13	Affiliation of author(s): AHTD, ADTG, VSSC, Thiruvananthapuram – 695 022					
14	Corporate author(s)					
15	Originating Unit: Vikram Sarabhai Space Centre, Thiruvananthapuram					
16	Sponsors: Name: Vikram Sarabhai Space Centre; Type: Government					
17	Date of Preparation: 14 09 2010			18	Date of Publication: 14 09 2010	
19	Publisher / Distributor: ADTG					
20	Form of Distribution: Hard Copy					
21	Language of Text: English			22	Language of Summary: English	
23	Number of Reference(s): 25			24	Gives data on: OTAP	
25	**Abstract:** *This report brings out features of the TPS design code OTAP (One-dimensional Thermal Analysis Package).*					
26	Keywords: OTAP, Aerodynamic heating, Thermal response and TPS.					
27	Class No.:			28	Supplementary elements:	

Acknowledgements

The work on 'OTAP' was carried out under the guidance of Dr. T. S. Prahlad. The package with capabilities for computing aerodynamic heating, thermal response analysis and Thermal Protection System design for ascent flight, was developed with contributions from Dr. M. S. Sastry, Shri. A. K. Verma, Dr. R. Balu, Dr. Pradeep Kumar, Dr. George Joseph and Shri. R. Swaminathan. The members of the task team acknowledge the contribution and express their gratitude to the team, which developed 'OTAP'.

The relentless contributions, support and reviews by Shri. R. Swaminathan (Chairman, Task Team) has been the key towards the release of OTAP users manual.

Thanks are also due to Dr. C. Unnikrishnan and V. Ashok of ARD for supplying the CFD data for validation of the design code.

The members of task team wish to acknowledge the motivation and encouragement rendered by Dr. K. Sivan, DD, AERO, Shri. S. V. Sharma, former DD, AERO, Dr. George Joseph, GD, ADTG and Shri. M. J. Chacko, Head, AHTD.

Contents

List of Tables

List of Figures

List of Appendices

AERODYNAMIC HEATING EVALUATION AND THERMAL PROTECTION SYSTEM DESIGN FOR SPACE VEHICLES

Abstract

This report brings out features of the TPS design code OTAP (One-dimensional Thermal Analysis Package). This code uses engineering methods for calculating the aerodynamic heat flux over space vehicles during their atmospheric flight. Thermal response of the structure is evaluated by solving one dimensional conduction equation locally for a multi layer structure with suitable boundary conditions, with provisions for charring/ablation/melting at the surface. This code can be used as a tool for the design of thermal protection system for ascent vehicles and re-entry modules.

1. INTRODUCTION

During atmospheric flight which includes ascent as well as re-entry into atmosphere, space vehicles encounter severe thermal environment. The kinetic energy of air is converted into thermal energy and part of this energy is transferred to the body by viscous diffusion. This is known as **Aerodynamic heating**. It is important that the structure, payload and other sensitive equipments are protected from excessive heating by means of a suitable Thermal Protection System (TPS). Design of TPS is a critical aspect of re-entry vehicle design.

Aerodynamic heating analysis involves evaluation of heat flux on the body due to air flow and the thermal response of the structure to this heat flux. These two problems are strictly coupled since the wall conditions affect the flow and vice versa. In practice, these two problems are solved separately in an iterative manner, till the process converges to a consistent solution.

2. CONVECTIVE HEAT TRANSFER

Theoretically, convective heat transfer can be estimated by solving the Navier-Stokes equations, which completely describe the flow field over a body using the conservation laws of mass, momentum and energy. These equations are extremely complex and their numerical solution requires large computer resources. Alternately, when the viscous-inviscid interactions are not strong, one can obtain the flow field from an inviscid, Euler code **[1]** and use this as input to a Boundary layer code **[2]** to evaluate the heat flux. These solutions have to be iteratively solved when interactions are predominant. However for design purposes, one can employ approximate methods based on Boundary Layer Theory. These methods give fairly accurate and conservative estimates of heat transfer over a wide range of flow conditions.

2.1 Thermal Design of Reentry Vehicles

Reentry vehicles experience very high velocities and heating rates compared to ascent vehicles. Hypersonic flows are characterized by the following features:

a) Real gas effects

Gas temperatures after the shock are very high. The perfect gas relations can be used for temperatures up to 1500 K. Beyond this temperature, molecular excitations start. Dissociation of oxygen starts around 2000 K and that of nitrogen starts around 4000 K. Around 4000 K, ionization of oxygen atoms starts and ionization of nitrogen starts around 8000 K. In between certain recombination reactions also take place. A lot of energy changes take place along with these reactions. The constituent gases of the air are in dissociated or ionized state. The flow can be in a chemically equilibrium (infinite reaction rates) or non equilibrium (finite reaction rates) or frozen (no reactions) state depending on the air density and temperature. Roughly the flow may be in chemically frozen state above 80 km. It may be in non-equilibrium state between 80 and 60 km and in equilibrium state between 60 and 40 km. The actual conditions depend on configuration and trajectory. At these elevated temperatures, the thermo physical and transport properties of a gas mixture vary drastically with temperature and pressure. Perfect gas assumptions are no longer valid.

b) Viscous shock layer

The entire shock layer becomes viscous. There is no clear demarcation between inviscid and viscous (boundary layer) regions.

c) Slip conditions

At high altitudes, the flow becomes rarefied. Continuum hypothesis is strictly not valid. Velocity and temperature show a jump close to the wall. A similar jump occurs at the shock also. Numerical solution of the conservation equations should include the effect of slip boundary conditions. Alternately, one can use Monte-Carlo simulations for estimating the heat transfer in the rarefied regime.

d) Radiation

Radiation from the hot gases in the shock layer to the body is significant for high speed flows (velocities more than 10 km/s). This radiation is likely to heat the free stream and changes free stream conditions. Radiation from the shock layer is significant for planetary entry bodies (like Jupiter) or earth reentry bodies from outer planets. At these entry velocities, the gases in the shock layer are in chemically and thermally non-equilibrium state.

e) Wall catalysis

A fully catalytic wall promotes recombination reactions, enhancing the wall heat transfer considerably. Therefore re-entry vehicles are generally provided non-catalytic coating to bring down the wall heat transfer.

f) Diffusion

Molecular diffusion also plays a role in changing the concentrations of the various species of gases.

All these effects influence the process of heat transfer to the wall significantly. To estimate the heat transfer accurately, one can use a viscous shock layer code **[3]** or non-equilibrium N-S Code **[4]**. But these codes cannot be used for routine design computations, as they require a lot of computer time. In the present formulation, simple, reasonably accurate engineering methods are used.

3. FORMULATION

In the present formulation, aerodynamic heating rates are computed using engineering methods based on the local inviscid flow properties. Where ever possible, the inviscid flow field obtained from CFD or wind tunnel measurements is read as an input. Where ever such inputs are not available, approximate inviscid flow properties are computed by the code.

3.1 Shock Relations

At supersonic speeds, a shock wave is formed over the body, causing an abrupt change in the flow properties. An attached oblique shock is formed in the case of sharp nosed bodies (up to a certain value of the vertex angle) like wedges and cones. A detached bow shock is formed in the case of blunt bodies. Rankine-Hugoniot relations are used to compute the properties across the shock when perfect gas assumptions hold good. For high temperature flows, one dimensional conservation equations are solved using equilibrium air properties from Hansen's tables. In the case of blunt bodies, normal shock relations may be assumed in the vicinity of the stagnation point. Since the heat transfer to the body depends on the properties of the body streamlines, this assumption is justified. Once the properties across the normal shock are known, flow variables on the body are estimated by using isentropic relations along the body streamline. This assumption may not strictly hold for hypersonic flows, since entropy changes occur over the body.

3.2 Approximate Inviscid Flow Field Calculation Methods

i. For supersonic flows over blunt bodies, normal shock relating (with equilibrium air properties) are used for computing the stagnations conditions (P_o, T_o). Newtonian pressure distributions are used along with isentropic relations to get the local flow properties (P_e, T_e, M_e) ***(Appendix-A1)***.

ii. For subsonic flows, potential flow is assumed for calculating the pressure distribution over the spherical cap and cylinder. Elsewhere free stream conditions are assumed ***(Appendix-A2)***.

iii. For supersonic flow over sharp wedges, oblique shock relations are used to get the local properties (P_e, T_e, M_e) ***(Appendix-A3)***. If the shock is detached, Newtonian pressure distribution is used to get the local properties.

iv. For supersonic flows over cones, the inviscid pressure is obtained from curve fits for the cone tables ***(Appendix-A2)***. Local Mach number is calculated from the stagnation pressure (after normal shock) and the local pressure using isentropic relations..

3.3 Engineering Heat Transfer Calculation Methods

i. Stagnation point heat transfer is calculated using the Fay and Riddell formula **[5]** ***(Appendix-A4)***. This formula requires the velocity gradient at the stagnation point. This formula is based on boundary layer method for flows in chemical equilibrium/non-equilibrium. This formula also accounts for the molecular diffusion taking place within the boundary layer. The velocity gradient at the stagnation point is an important parameter in this formula. For supersonic flows over a sphere or cylinder, it can be based on Newtonian pressure distribution. For highly blunt body configurations, the experimental velocity gradients can be used **[6]**. Velocity gradient at the stagnation point of the blunt bodies is shown in **Fig. 1, 2 & 3**. For highly blunt bodies like re-entry capsules (where R >> r), stagnation point velocity gradient is shown in **Fig. 4**. It is seen from the **Fig. 5** that for large values of R, the velocity gradient reaches the value for flat headed cylinder asymptotically.

ii. Laminar heat transfer in the stagnation region is calculated using the Lees formula **(Appendix-A5)** **[7]**. This formula is applicable for the spherical and conical regions.

iii. Heat transfer on the cone and cylinder are computed using the Van-Driest formulas for laminar and turbulent flows based on the local Reynolds number **(Appendix-A6)** **[8]**. This formula is based on boundary layer flow over a flat plate. Cone rule is applied for correcting the Van-Driest formula for conical flow. The local Reynolds number is reduced by a factor of 3 for laminar flow and a factor of 2 for turbulent flow. No correction is given for the cylindrical part. The heat transfer rates from Van-Driest formula generally compare well with boundary layer or Navier-Stokes solutions. For re-entry heat flux estimation on cone and flare regions (aft-bodies), Eckert formula **(Appendix-A7)** **[9]** is used.

iv. Transition is assumed to begin when the local Reynolds number exceeds 10^6 (or the Reynolds number based on momentum thickness Re_θ exceeds 300^o). Chen and Thyson correlation **(Appendix-A8)** **[10]** is used for calculating the transitional phase between laminar and turbulent flow. A weighted average is taken based on the intermittency factor. For ascent vehicles, the flow becomes turbulent right on the nose cap and remains fully turbulent roughly up to 50 km. For reentry vehicles, the flow is laminar from 120 km to about 30 km. Transition studies are more important for re-entry vehicles which experience very high heating rates.

v. For flows with angle of incidence, the body is treated as an infinite swept cylinder. Heat transfer along the windward generator is calculated using Beckwith and Gallagher's formula **(Appendix-A9)** **[11]**. The laminar formula involves cos λ factor. The turbulent formula involves a product of cos λ and sin λ factors. Both the formula gives zero heat transfer as $\lambda \rightarrow 90°$. The turbulent formula gives a peak value for $\lambda = 30°$. When the sweep angle $\lambda = 0$ and flow is laminar, heating is maximum. But the turbulent formula gives zero heat transfer when $\lambda = 0$. Therefore in the computations, care must be taken to switch over to the laminar formula when $\lambda < 10$.

vi. For rarefied flows, heat transfer is computed by taking a weighted average between continuum and free molecular values, the weighing factor being based on the Knudsen number. Continuum values are used for $Kn < 0.01$, Free molecular formula is used for $Kn > 10$ and transitional flow is assumed in between **(Appendix-A10)** **[12, 13]**. This approach covers the slip regime also.

3.4 Heat transfer in the shock-boundary layer interaction zone and over protrusions

Whenever shocks interact with the boundary layer (eg: Strapon core region of launch vehicles, fuselage wing junctions in RLV, fin body interface in sounding rockets, wing elevon interface) the local heat transfer coefficient needs to be augmented. From the literature, it is seen these augmentation factors can be used for design.

$$\frac{h}{h_o} = \begin{cases} \left(\dfrac{P_1}{P_2}\right)^{0.5}, \text{Laminar flow} \\ \left(\dfrac{P_1}{P_2}\right)^{0.8}, \text{Turbulent flow} \end{cases}$$

where $\frac{P_1}{P_2}$ is the static pressure ratio across such shocks. Similar factors can be used for protrusions also.

4. RADIATION HEAT TRANSFER

The net heat transfer to the body is computed by subtracting the radiation loss to the surroundings, from the convective heat transfer. Heat loss to the ambient is given by $q_{rad} = \varepsilon\, \sigma\, (T_w^4 - T_{amb}^4)$, where ε is the emissivity of the wall and σ is Stefan-Boltzmann constant. T_{amb} is the ambient temperature.

Solar radiation also gives heat input for the body, especially in the upper atmosphere or during orbital phase of a space vehicle; where there is practically no convective heating. The radiative equilibrium temperature attained by the vehicle is given by, $\varepsilon\, \sigma\, T^4 = \alpha_s\, (E_s + E_r + E_d)$ where E_s is the solar radiation (0.1353 W/cm^2), E_r is is the reflected solar radiation (0.0234 W/cm^2) and E_d is the Earth's re-radiation (0.0208 W/cm^2). Thus the radiative equilibrium temperature is dependent on the absorptivity α_s and the emissivity ε.

At speeds more than the orbital velocities, (as in the case of re-entry from other planets), radiation from the hot gases of the shock layer to the body becomes significant. The radiation from the gases is given by the empirical formulae [14].

$$q_{rad} = 100 r_N \left(\frac{V}{10,000}\right)^{8.5} \left(\frac{\rho_\infty}{\rho_{SL}}\right)^{1.6} \; BTU / ft^2 / \sec$$

where r_N is the nose radius in feet, V is the free stream velocity ft/s, ρ_∞ is the free stream density and ρ_{SL} is the sea level density.

5. FREE CONVECTION HEAT TRANSFER

While computing the thermal response of the structure, convective heat transfer from the inner surface is to be considered. The following free convection formula is used for estimating the heat transfer coefficient on the inner boundary **(Appendix-A11)** **[15]**.

$$Nu = \begin{cases} 0.59\,(Gr\,\mathrm{Pr})^{1/4} & (Gr\,\mathrm{Pr} < 10^9) \\ 0.13\,(Gr\,\mathrm{Pr})^{1/3} & (Gr\,\mathrm{Pr} > 10^9) \end{cases}$$

$$\mathrm{Gr} = \frac{\mathrm{g}\,\Delta \mathrm{T}\,\mathrm{L}^3\,\rho^2}{\bar{\mathrm{T}}\mu^2}$$

where $\Delta \mathrm{T} = \mathrm{T} - \mathrm{T}_{amb}$ and $\bar{\mathrm{T}} = \frac{(\mathrm{T} + \mathrm{T}_{amb})}{2}$

6. CONDUCTION HEAT TRANSFER

Aerodynamic heating analysis involves evaluation of heat flux on the body due to air flow and the thermal response of the structure to this heat flux. These two problems are strictly coupled since the wall conditions affect the flow and vice versa. In practice, these two problems are solved separately in an iterative manner, till the process converges to a consistent solution.

6.1 One dimensional thermal response of a multi-layer Thermal Protection System with Charring/ Ablation at the surface

The governing equation for the **Char layer** is

$$\rho_1 C_1 \frac{\partial T_1}{\partial t} = \frac{\partial}{\partial y}\left(k_1 \frac{\partial T_1}{\partial y}\right) + \dot{m}_p C_1 \frac{\partial T_1}{\partial y} \qquad (1)$$

$$(\bar{x} \le y \le \bar{x} + x_1)$$

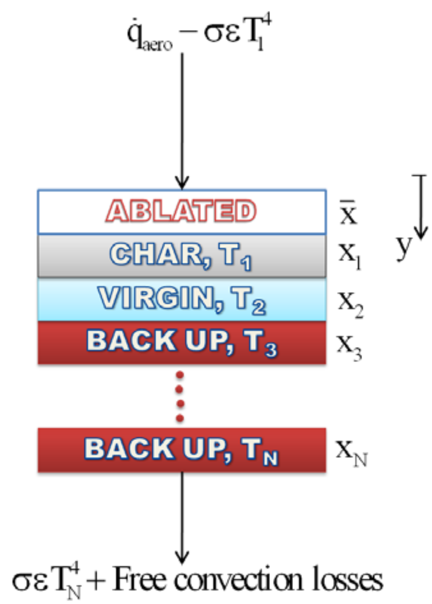

Boundary conditions are

$$y = \bar{x} = \int_0^t \frac{\dot{m}_a \, dt}{\rho_1} \qquad (2)$$

$$\dot{q}_{aero} = \sigma\varepsilon T_1^4 - k_1 \frac{\partial T_1}{\partial y} + U(T_1 - T_A)\dot{m}_a H_a \qquad (3)$$

where T_A is the ablation temperature and U is the unit step function.

$$U = \begin{cases} 0, \text{ when } T_1 < T_A \\ 1, \text{ when } T_1 \ge T_A \end{cases}$$

From equation (3), $\dot{m}_a$ is calculated and from equation (2) $\bar{x}$ is calculated.

H_a is the heat of ablation.

$\dot{m}_a$ is the ablation mass rate/area.

$$\text{At } y = \bar{x} + x_1, T_1 = T_2 = T_p \qquad (4)$$

T_p is the pyrolysis temperature at the Char/virgin interface. Since the interfaces move with time during the process of ablation/charring, the governing equation is written in moving co-ordinate system so that interface conditions are specified easily. Char thickness is given by

$$x_1 = x_1(t=0) + \int_0^t \frac{\dot{m}_p \, dt}{(\rho_2 - \rho_1)} - \int_0^t \frac{\dot{m}_a \, dt}{\rho_1} \qquad (5)$$

$$-k_1 \frac{\partial T_1}{\partial y} = -k_2 \frac{\partial T_2}{\partial y} + U(T_2 - T_p)\dot{m}_p H_p \qquad (6)$$

where T_p is the pyrolysis temperature and H_p is the heat of pyrolysis. U is the unit step function. $\dot{m}_p$ is calculated from equation (5)and x_1 is calculated from (4)

Virgin thickness is given by

$$x_2 = x_2(t=0) - \int_0^t \frac{\dot{m}_p}{(\rho_2 - \rho_1)} dt \qquad (7)$$

The governing equation for the **virgin layer** is

$$\rho_2 C_2 \frac{\partial T_2}{\partial t} = \frac{\partial}{\partial y}\left(k_2 \frac{\partial T_2}{\partial y}\right) \quad (\overline{x} + x_1 \le y \le \overline{x} + x_1 + x_2) \qquad (8)$$

Boundary Conditions are

At $y = \overline{x} + x_1, \quad T_1 = T_2 = T_p$

$$-k_1 \frac{\partial T_1}{\partial y} = -k_2 \frac{\partial T_2}{\partial y} + U(T_2 - T_p)\dot{m}_p H_p \qquad (9)$$

At $y = \overline{x} + x_1 + x_2, \quad k_2 \frac{\partial T_2}{\partial y} = k_3 \frac{\partial T_3}{\partial y}$ (10)

The governing equation for **other layers** is

$$\rho_i c_i \frac{\partial T_i}{\partial t} = \frac{\partial}{\partial y}\left(k_i \frac{\partial T_i}{\partial y}\right) \quad (i = 3, \ldots\ldots\ldots N) \qquad (11)$$

with the interface conditions:

$$T_i = T_{i-1} \quad \text{and} \quad k_{i-1} \frac{\partial T_{i-1}}{\partial y} = k_i \frac{\partial T_i}{\partial y}$$

At the last layer, free convection and radiation conditions are imposed at the inner boundary.

The boundary conditions are put in the general form

$$A_1 \frac{\partial T}{\partial x} + A_2 \frac{\partial T}{\partial t} + A_3 T = A_4 \qquad (12)$$

By defining A1, A2, A3 and A4 appropriately boundary conditions of the various forms can be obtained (convective, radiative, temperature specified and mixed).

The governing equations for all layers are solved together along with the interface and boundary conditions using implicit central difference scheme **[16]**. The resulting discretized algebraic equations are tri-diagonal in nature and are solved by a standard procedure (forward sweep and backward substitution) **[17, 18]**.

7. Design Cycle

The inputs required for the thermal design and analysis are:

a) Vehicle configuration (geometry).
b) Inviscid flow field data (whenever applicable).
c) Trajectory (Variation of altitude and relative velocity with time).
d) Material properties.
e) Nominal Indian Atmosphere 2002 ***(Table 1)*** **[19]**.
f) Equilibrium air properties: The air properties in general depend on the state of the chemical reactions that are taking place. However in the present formulation, only equilibrium heating rates are computed, as they are expected to give conservative estimates for design. Hansen's equilibrium air property model **[20]** which gives various thermodynamic and transport properties of air as function of temperature and pressure is built into the program. The data is presented in ***Tables 2, 3, 4, 5, 6, 7 and 8***. External TPS design criteria adopted is described in Annexure –B1:

8. PROGRAM OTAP

Figures 6 & 7 show the flow chart of OTAP program for heat flux computation and thermal response & TPS design respectively. This section gives details on various input variables, subroutines and output variables for OTAP program.

8.1 Input Variables

Input variables include input cards, geometry description variables, trajectory variables, solution parameters and perturbation/augmentation factors. The significance of all input variables to carry out thermal response analysis is discussed in **Appendix A12.**

8.2 List of Subroutines

OTAP software consists of a main program with various subroutines. The functions performed by various modules are described in **Appendix A13.**

8.3 Output Variables

The output variables are described in **Appendix A14**.

A sample of input and output files is given in **Appendix A15**.

9. VALIDATION

In order to check the validity of the methods for predicting heat transfer rates, cold wall heat flux distribution computed using the design code 'OTAP' has been compared with those obtained from various sources. The wall temperature is taken as 300 K, for purposes of comparison. The details of these validations are given in the following sections **[21, 22]**:

9.1 Published Data from Calspan 96-in Shock Tunnel

A laboratory measurements program, performed in the Calspan 96-in Hypersonic Shock Tunnel, provides a database for a re-entry sphere cone configuration with a nose radius of 43.2 mm and a cone angle of 7.8 degrees. The test conditions are : Total temperature of 6000 K, total pressure of 500 atmospheres and Mach Number of 9.3. **Figure 6** gives the comparison of Calspan Shock Tunnel data with the data computed using the present program. The agreement is fairly good.

9.2 CFD Computations Using 'UNS2D'

Laminar heat flux distribution over SRE Module for various flow conditions were computed using a Navier-Stokes solver 'UNS2D' where equilibrium air properties were considered. The results computed using 'OTAP' and 'UNS2D' are compared. Figure 7 shows the comparison of heat flux for M = 15 and altitude 42 km and there is fairly good agreement between the results.

9.3 CFD Computations Using 'PARAS-3D'

Heat flux distribution over SRE for M=20.0 and altitude 51 km computed using 'OTAP' and 'PARAS-3D' is compared in figure 8. It is seen that 'OTAP' heat flux values are marginally higher than fully catalytic heat flux values computed using 'PARAS-3D', on the spherical cap whereas these are marginally lower on the cone and flare.

9.4 Comparison with various flight measurements

Design software code OTAP has been used for estimation of heat flux and thermal response on Heat Shield of GSLV FO4 and silica tile of SRE 1 mission. A fairly good comparison between the measured and computed temperatures as shown in **Figures 9, 10, 11and 12** validates design code OTAP.

10. CONCLUDING REMARKS

A detailed reference manual for OTAP (One-dimensional Thermal Analysis Package) has been brought out. It includes details on different engineering methods used for heat flux estimation for various geometries. Thermal response of a multi-layer TPS (charring/ablating surface) with boundary conditions is described with mathematical formulation.

Design cycle and the philosophy adopted for TPS design of launch vehicles and re-entering modules are also addressed in this manual.

List of different subroutines used in the program along with significance of input variables, output variables is described. Sample input and sample output calculations using the program are also included in this reference manual.

References

1. *K. P. Singh et. al,* “Numerical Simulation of Three Dimensional Inviscid Supersonic Flow Over Launch Vehicle”, *VSSC:TR:02:214:80, 1980*.
2. *R. Balu and R. Swaminathan*, “Development of a Fast Boundary Layer Package for Aerodynamic Heating Applications”, *SSTC-ARD-Feb (2), 1982.*
3. *S Swaminathan*, “Three-Dimensional Non equilibrium Viscous Shock Layer Flows over Reentry Vehicles”, *Ph.D Thesis, VPI & S.U; USA 1983.*
4. *Pradeep Kumar,* “Navier Stokes for Hypersonic Viscous Non-equilibrium Flow over the Stagnation region of a Blunt Body”, *Ph.D Thesis, IIT Kanpur 1989.*
5. *F. A. Fay and F. R. Riddell,* “Theory of Stagnation Point Heat Transfer in Dissociated Air”, *Journal of Aeronautical Science, Vol. 25, 1958*.
6. *F. M. White,* “Viscous Flow”, McGraw Hill, 1974
7. *Lees. L,* “Laminar Heat Transfer over Blunt Nosed Bodies at Hypersonic Flight Speeds”, *Jet Propulsion, Vol 26, 1956.*
8. *Van Driest E. R*; “Investigation of Laminar Boundary Layer in Compressible Fluids Using the Cross Method”, NACA TN 2597, 1957. Curve fits from NASA-TMX-2058.
9. *E. R. G. Eckerts*,” Engineering Relations for Heat Transfer and friction in High Velocity Laminar and Turbulent Boundary Layer Flow Over Surface with Constant Pressure and Temperature,” J Aerospace Science, Vol. 22(August 1955)
10. *Chen K. K and Thyson A,* “Extension of Emmons Spot Theory to Flows on Blunt Bodies”, AIAA Journal, Vol 19,1971.
11. *Beckwith C. E and Gallagher J. J,* “ Local Heat Transfer and recovery temperature on a Yawed Cylinder at a Mach number of 4.15 and at High Reynolds Number, NASA-TR- R-104, 1961.
12. *Reeves B. L,* “Aerodynamic Heating in the Slip, Intermediate and Free molecular Flow Regimes”, Report No: 6859, Mc Donnel Dongles Aircraft Corporation, 1959.
13. *Rohsenow and Hartnelt,* Handbook of Heat transfer, McGraw Hill, 1973.
14. *Detra, R. W. and Hidalgo, H*, “Generalized Heat Transfer Formulas and Graphs for Nose Cone Re-entry into the Atmosphere”, ARS Journal.
15. *Irwin and Hartnell,* “Advances in Heat Transfer”, Vol. II, A P 1965.

16. *Swan R. T, Pittman C. M and Smith J. C*, “One dimensional Numerical Analysis of the Transient Response of Thermal Protection Systems”, NASA TN D 2976, 1965.
17. *S. V. Patankar,* “A Numerical Method for Conduction in Composite Materials Flow in Irregular Geometries and Conjugate Heat Transfer”, Proceedings of Sixth International Heat Transfer Conference, 3, 297-, Toronto, 1978.
18. *S. V. Patankar, Balinga B. R.,* “A New Finite Difference Scheme for Parabolic Differential Equations”, Journal of Numerical Heat Transfer, I, 27 – 37, 1978.
19. *George Joseph et al.,* “A Reference Indian Atmosphere Model From 0 to 1000 Kilometers”, VSSC/AHTD/SP/01/2002.
20. *C.F. Hansen,* “Thermodynamic and Transport Properties of High Temperature Air” NASA TR -R -50, 1959.
21. *George Joseph, R. Swaminathan and Sundar. B,* “RETAP – A Software for Aerodynamic Heating Analysis and Thermal Protection System Design of Re-entry Vehicles”, VSSC/ATG/TR/001/2003.
22. Sundar. B et. al., “Comprehensive Design Review on Aerothermal Design Analysis and Qualification of SRE Module”, VSSC/ADTG/TM-SRE/001/2006.
23. George Joseph, “Thermal Protection Requirement in the Vicinity of Protuberances”, VSSC/AHTD/TN-GSLV/001/1998.
24. *A. K. Verma et. al.,* “Thermal Design and Analysis of GSLV – CDR Report”, VSSC/AHTD/TM-GSLV/054/99.
25. *A. K. Verma et. al.,* “Aerothermal Design of PSLV-CDR Report”, AHTS/PN/22/1992.

TABLE - 1

Nominal Indian Atmosphere 2002

Altitude (km)	Temperature (K)	Pressure (Pa)	Density (kg/m^3)	Altitude (km)	Temperature (K)	Pressure (Pa)	Density (kg/m3)
0	300.7	1.01E+05	1.17E+00	39	254.2	3.48E+02	4.77E-03
1	294.6	9.00E+04	1.06E+00	40	256.6	3.05E+02	4.14E-03
2	288.4	8.01E+04	9.67E-01	41	258.9	2.68E+02	3.60E-03
3	283.6	7.11E+04	8.73E-01	42	260.6	2.35E+02	3.14E-03
4	278.4	6.30E+04	7.88E-01	43	262	2.07E+02	2.75E-03
5	272.9	5.57E+04	7.11E-01	44	262.9	1.82E+02	2.41E-03
6	267.2	4.91E+04	6.40E-01	45	263.8	1.60E+02	2.12E-03
7	261.4	4.31E+04	5.75E-01	46	264.4	1.41E+02	1.86E-03
8	254.9	3.78E+04	5.17E-01	47	264.7	1.24E+02	1.64E-03
9	247.9	3.30E+04	4.64E-01	48	264.6	1.09E+02	1.44E-03
10	240.4	2.87E+04	4.17E-01	49	264.1	9.64E+01	1.27E-03
11	232.4	2.49E+04	3.73E-01	50	263.5	8.49E+01	1.12E-03
12	224.2	2.15E+04	3.33E-01	51	262.5	7.47E+01	9.92E-04
13	215.9	1.84E+04	2.97E-01	52	261	6.57E+01	8.78E-04
14	207.7	1.57E+04	2.63E-01	53	258.9	5.78E+01	7.78E-04
15	200.8	1.33E+04	2.30E-01	54	256.4	5.07E+01	6.89E-04
16	195.6	1.12E+04	1.99E-01	55	253.6	4.45E+01	6.11E-04
17	194.2	9.40E+03	1.69E-01	56	251.1	3.90E+01	5.41E-04
18	197.3	7.90E+03	1.40E-01	57	248.5	3.41E+01	4.78E-04
19	201.7	6.67E+03	1.15E-01	58	245.3	2.98E+01	4.23E-04
20	206.6	5.65E+03	9.53E-02	59	241.7	2.59E+01	3.74E-04
21	209.1	4.80E+03	7.99E-02	60	238	2.26E+01	3.30E-04
22	212.2	4.09E+03	6.71E-02	61	234.1	1.96E+01	2.91E-04
23	215.5	3.49E+03	5.64E-02	62	230.3	1.70E+01	2.57E-04
24	218.8	2.99E+03	4.75E-02	63	226.9	1.47E+01	2.25E-04
25	221.3	2.56E+03	4.03E-02	64	223.5	1.26E+01	1.97E-04
26	223.8	2.20E+03	3.42E-02	65	220.4	1.09E+01	1.72E-04
27	226	1.89E+03	2.92E-02	66	217.3	9.33E+00	1.50E-04
28	228	1.63E+03	2.49E-02	67	213.9	7.99E+00	1.30E-04
29	230.3	1.41E+03	2.13E-02	68	210.2	6.83E+00	1.13E-04
30	232.4	1.22E+03	1.82E-02	69	207.3	5.82E+00	9.78E-05
31	234.4	1.05E+03	1.56E-02	70	204.8	4.95E+00	8.42E-05
32	236.3	9.12E+02	1.34E-02	71	203.5	4.20E+00	7.20E-05
33	238.4	7.91E+02	1.16E-02	72	201.7	3.57E+00	6.16E-05
34	240.7	6.87E+02	9.95E-03	73	199.5	3.02E+00	5.28E-05
35	243.4	5.98E+02	8.56E-03	74	197	2.56E+00	4.49E-05
36	246.1	5.21E+02	7.38E-03	75	194.4	2.16E+00	3.87E-05
37	248.9	4.55E+02	6.36E-03	76	193.4	1.82E+00	3.27E-05
38	251.7	3.98E+02	5.50E-03	77	191.4	1.53E+00	2.78E-05

Altitude (km)	Temperature (K)	Pressure (Pa)	Density (kg/m^3)
78	190.6	1.28E+00	2.35E-05
79	188.4	1.08E+00	1.99E-05
80	187.1	9.03E-01	1.68E-05
81	185.6	8.51E-01	1.48E-05
82	184.1	7.18E-01	1.25E-05
83	182.8	6.06E-01	1.06E-05
84	181.5	5.11E-01	9.01E-06
85	180.3	4.30E-01	7.64E-06
86	179.2	3.62E-01	6.47E-06
87	178.2	3.04E-01	5.48E-06
88	177.3	2.55E-01	4.64E-06
89	176.5	2.14E-01	3.92E-06
90	175.7	1.79E-01	3.32E-06
91	175	1.49E-01	2.80E-06
92	174.5	1.24E-01	2.36E-06
93	174	1.04E-01	1.99E-06
94	173.6	8.60E-02	1.67E-06
95	173.3	7.14E-02	1.40E-06
96	173.1	5.92E-02	1.16E-06
97	173	4.90E-02	9.67E-07
98	172.9	4.07E-02	8.00E-07
99	173.4	3.37E-02	6.60E-07
100	174.8	2.81E-02	5.43E-07
101	177.1	2.34E-02	4.45E-07
102	180.4	1.96E-02	3.65E-07
103	184.7	1.65E-02	2.99E-07
104	189.9	1.39E-02	2.45E-07
105	196	1.18E-02	2.01E-07
106	203	1.01E-02	1.65E-07
107	210.9	8.70E-03	1.36E-07
108	219.8	7.54E-03	1.13E-07
109	229.5	6.58E-03	9.39E-08
110	239.9	5.78E-03	7.85E-08
111	251	5.11E-03	6.61E-08
112	262.7	4.54E-03	5.59E-08
113	275	4.06E-03	4.76E-08
114	288	3.65E-03	4.07E-08
115	301.6	3.30E-03	3.50E-08
116	315.8	3.00E-03	3.02E-08
117	330.5	2.74E-03	2.63E-08
118	345.8	2.51E-03	2.29E-08
119	361.4	2.31E-03	2.01E-08
120	377.3	2.14E-03	1.78E-08
121	393.3	1.98E-03	1.58E-08
122	409.1	1.85E-03	1.40E-08
123	424.6	1.72E-03	1.26E-08
124	439.7	1.61E-03	1.13E-08
125	454.4	1.51E-03	1.03E-08
126	468.7	1.42E-03	9.31E-09
127	482.6	1.34E-03	8.49E-09
128	496.2	1.26E-03	7.77E-09
129	509.4	1.19E-03	7.13E-09
130	522.3	1.13E-03	6.57E-09
131	534.8	1.07E-03	6.06E-09
132	547.1	1.02E-03	5.61E-09
133	559	9.67E-04	5.20E-09
134	570.6	9.20E-04	4.84E-09
135	581.9	8.76E-04	4.51E-09
136	592.9	8.35E-04	4.21E-09
137	603.6	7.97E-04	3.94E-09
138	614.1	7.62E-04	3.69E-09
139	624.3	7.28E-04	3.46E-09
140	634.2	6.97E-04	3.25E-09
141	643.9	6.68E-04	3.06E-09
142	653.3	6.40E-04	2.88E-09
143	662.5	6.14E-04	2.72E-09
144	671.4	5.89E-04	2.57E-09
145	680.1	5.66E-04	2.43E-09
146	688.6	5.44E-04	2.30E-09
147	696.9	5.23E-04	2.18E-09
148	705	5.03E-04	2.07E-09
149	712.8	4.84E-04	1.96E-09
150	720.5	4.66E-04	1.87E-09
151	727.9	4.49E-04	1.78E-09
152	735.2	4.33E-04	1.69E-09
153	742.3	4.17E-04	1.61E-09
154	749.2	4.03E-04	1.54E-09
155	755.9	3.89E-04	1.47E-09
156	762.5	3.75E-04	1.40E-09
157	768.8	3.62E-04	1.34E-09
158	775.1	3.50E-04	1.28E-09
159	781.1	3.39E-04	1.23E-09
160	787	3.27E-04	1.17E-09
161	792.8	3.17E-04	1.13E-09
162	798.4	3.06E-04	1.08E-09
163	803.9	2.97E-04	1.03E-09
164	809.2	2.87E-04	9.93E-10
165	814.4	2.78E-04	9.53E-10

Altitude (km)	Temperature (K)	Pressure (Pa)	Density (kg/m^3)
166	819.4	2.69E-04	9.15E-10
167	824.4	2.61E-04	8.80E-10
168	829.2	2.53E-04	8.46E-10
169	833.9	2.45E-04	8.14E-10
170	838.4	2.38E-04	7.83E-10
171	842.9	2.31E-04	7.54E-10
172	847.2	2.24E-04	7.26E-10
173	851.4	2.17E-04	7.00E-10
174	855.5	2.11E-04	6.75E-10
175	859.6	2.05E-04	6.51E-10
176	863.5	1.99E-04	6.27E-10
177	867.3	1.93E-04	6.05E-10
178	871	1.88E-04	5.84E-10
179	874.6	1.82E-04	5.64E-10
180	878.1	1.77E-04	5.45E-10
181	881.6	1.72E-04	5.27E-10
182	884.9	1.67E-04	5.09E-10
183	888.2	1.63E-04	4.92E-10
184	891.4	1.58E-04	4.76E-10
185	894.5	1.54E-04	4.60E-10
186	897.5	1.50E-04	4.45E-10
187	900.4	1.46E-04	4.31E-10
188	903.3	1.42E-04	4.17E-10
189	906.1	1.38E-04	4.04E-10
190	908.8	1.35E-04	3.91E-10
191	911.5	1.31E-04	3.79E-10
192	914.1	1.28E-04	3.67E-10
193	916.6	1.24E-04	3.56E-10
194	919.1	1.21E-04	3.45E-10
195	921.5	1.18E-04	3.34E-10
196	923.8	1.15E-04	3.24E-10
197	926.1	1.12E-04	3.15E-10
198	928.3	1.09E-04	3.05E-10
199	930.5	1.06E-04	2.96E-10
200	932.6	1.04E-04	2.87E-10
210	951	8.07E-05	2.15E-10
220	965.3	6.36E-05	1.64E-10
230	976.3	5.05E-05	1.26E-10
240	984.9	4.04E-05	9.79E-11
250	991.6	3.25E-05	7.68E-11
260	996.8	2.63E-05	6.08E-11
270	1000.8	2.14E-05	4.84E-11
280	1004	1.75E-05	3.89E-11
290	1006.4	1.43E-05	3.13E-11

Altitude (km)	Temperature (K)	Pressure (Pa)	Density (kg/m^3)
300	1008.3	1.18E-05	2.54E-11
310	1009.8	9.77E-06	2.07E-11
320	1011	8.10E-06	1.69E-11
330	1011.9	6.74E-06	1.39E-11
340	1012.6	5.62E-06	1.15E-11
350	1013.2	4.70E-06	9.50E-12
360	1013.6	3.94E-06	7.89E-12
370	1014	3.31E-06	6.57E-12
380	1014.2	2.79E-06	5.48E-12
390	1014.4	2.35E-06	4.58E-12
400	1014.6	1.99E-06	3.84E-12
410	1014.7	1.68E-06	3.23E-12
420	1014.8	1.43E-06	2.72E-12
430	1014.9	1.21E-06	2.29E-12
440	1015	1.03E-06	1.94E-12
450	1015	8.78E-07	1.64E-12
460	1015.1	7.49E-07	1.39E-12
470	1015.1	6.40E-07	1.18E-12
480	1015.1	5.49E-07	1.00E-12
490	1015.1	4.71E-07	8.50E-13
500	1015.2	4.05E-07	7.24E-13
510	1015.2	3.48E-07	6.18E-13
520	1015.2	3.01E-07	5.27E-13
530	1015.2	2.60E-07	4.51E-13
540	1015.2	2.25E-07	3.86E-13
550	1015.2	1.96E-07	3.31E-13
560	1015.2	1.70E-07	2.84E-13
570	1015.2	1.49E-07	2.44E-13
580	1015.2	1.30E-07	2.10E-13
590	1015.2	1.14E-07	1.81E-13
600	1015.2	1.00E-07	1.56E-13
610	1015.2	8.85E-08	1.34E-13
620	1015.2	7.83E-08	1.16E-13
630	1015.2	6.95E-08	1.01E-13
640	1015.2	6.20E-08	8.74E-14
650	1015.2	5.54E-08	7.60E-14
660	1015.2	4.97E-08	6.62E-14
670	1015.2	4.48E-08	5.78E-14
680	1015.2	4.04E-08	5.05E-14
690	1015.2	3.67E-08	4.43E-14
700	1015.2	3.34E-08	3.89E-14
710	1015.2	3.05E-08	3.43E-14
720	1015.2	2.80E-08	3.03E-14
730	1015.2	2.57E-08	2.68E-14

Altitude (km)	Temperature (K)	Pressure (Pa)	Density (kg/m^3)
740	1015.2	2.38E-08	2.38E-14
750	1015.2	2.20E-08	2.12E-14
760	1015.2	2.05E-08	1.89E-14
770	1015.2	1.91E-08	1.69E-14
780	1015.2	1.79E-08	1.52E-14
790	1015.2	1.68E-08	1.37E-14
800	1015.2	1.58E-08	1.24E-14
810	1015.2	1.49E-08	1.12E-14
820	1015.2	1.41E-08	1.02E-14
830	1015.2	1.33E-08	9.33E-15
840	1015.2	1.27E-08	8.55E-15
850	1015.2	1.20E-08	7.85E-15
860	1015.2	1.15E-08	7.24E-15
870	1015.2	1.10E-08	6.70E-15

Altitude (km)	Temperature (K)	Pressure (Pa)	Density (kg/m^3)
880	1015.2	1.05E-08	6.21E-15
890	1015.2	1.00E-08	5.78E-15
900	1015.2	9.63E-09	5.39E-15
910	1015.2	9.25E-09	5.04E-15
920	1015.2	8.90E-09	4.73E-15
930	1015.2	8.57E-09	4.45E-15
940	1015.2	8.26E-09	4.19E-15
950	1015.2	7.97E-09	3.96E-15
960	1015.2	7.69E-09	3.75E-15
970	1015.2	7.43E-09	3.56E-15
980	1015.2	7.19E-09	3.38E-15
990	1015.2	6.96E-09	3.21E-15
1000	1015.2	6.74E-09	3.06E-15

TABLE - 2

Variation of Cp (J/kg K) with Pressure & Temperature

Temp(K)	PRESSURE (atm)						
	100	10	1	0.1	0.01	0.001	0.0001
500	1030.3	1030.3	1030.3	1030.3	1030.3	1030.3	1030.3
1000	1136.5	1136.5	1136.5	1136.5	1136.5	1136.5	1136.5
1500	1205.4	1205.4	1205.4	1205.4	1208.3	1214.0	1231.2
2000	1245.6	1248.4	1265.7	1311.6	1463.7	1931.5	3320.6
2500	1294.4	1360.4	1567.0	2189.8	3897.5	6888.0	5748.6
3000	1443.6	1788.0	2760.9	4775.7	5068.4	2261.6	1552.7
3500	1799.5	2726.5	4276.3	3533.0	1868.4	1905.7	3068.0
4000	2364.9	3578.9	3171.4	1983.2	2436.6	4724.0	11703.9
4500	2904.4	3174.2	2189.8	2758.1	5648.2	14080.2	29127.6
5000	3022.1	2459.6	2749.5	5447.3	13265.1	25020.7	13629.6
5500	2743.7	2600.2	4548.9	10687.9	20864.9	12794.5	3679.3
6000	2597.4	3553.1	7734.7	16531.2	14169.2	4350.9	3280.4
6500	2884.4	5255.0	11804.3	15604.2	5912.2	3375.1	5490.3
7000	3587.5	7605.5	14235.2	8948.7	3699.4	4701.1	10567.3
7500	4729.8	10099.5	12252.0	4970.8	4015.1	7754.7	20095.7
8000	6147.5	11574.7	8113.5	3926.2	5567.8	13092.9	34899.2
8500	7662.9	10946.2	5332.5	4279.2	8279.9	21329.8	49754.3
9000	8911.4	8719.1	4256.2	5424.3	12372.6	31989.0	49742.8
9500	9442.3	6457.5	4204.6	7249.6	17992.0	41310.8	32993.5
10000	9020.4	5011.0	4744.1	9789.6	24805.4	42217.7	17303.2
10500	7881.0	4359.5	5699.8	13067.1	31380.6	32936.1	9181.1
11000	9419.3	4256.2	7020.0	17004.8	34950.9	21094.5	5717.0
11500	5441.5	4508.8	8687.5	21266.7	33142.8	12679.7	4284.9
12000	4703.9	5008.2	10685.0	25132.6	26800.1	8010.2	3679.3
12500	4307.9	5705.6	12963.8	27554.9	19332.3	5645.3	3412.4
13000	4181.6	6569.4	15411.9	27595.0	13302.5	4465.7	3291.9
13500	4247.6	7582.5	17828.4	25138.3	9270.1	3871.6	3231.6
14000	4454.2	8727.7	19920.7	21071.5	6807.6	3561.7	3202.9
14500	4769.9	9979.0	21341.3	16733.8	5355.4	3395.2	3185.7
15000	5171.7	11299.2	21797.7	12814.6	4505.9	3303.4	3180.0

TABLE-3

Variation of GAMA with Pressure & Temperature

Temp(K)	PRESSURE (atm)						
	100	10	1	0.1	0.01	0.001	0.0001
500	1.387	1.387	1.387	1.387	1.387	1.387	1.387
1000	1.337	1.337	1.337	1.337	1.337	1.337	1.337
1500	1.312	1.312	1.312	1.312	1.312	1.31	1.306
2000	1.3	1.299	1.296	1.286	1.26	1.209	1.153
2500	1.288	1.277	1.249	1.202	1.161	1.152	1.157
3000	1.266	1.235	1.195	1.178	1.181	1.239	1.304
3500	1.241	1.211	1.202	1.212	1.27	1.252	1.176
4000	1.23	1.223	1.23	1.26	1.213	1.15	1.133
4500	1.24	1.243	1.251	1.204	1.154	1.155	1.19
5000	1.256	1.252	1.212	1.166	1.172	1.203	1.168
5500	1.262	1.231	1.183	1.182	1.214	1.183	1.257
6000	1.253	1.206	1.19	1.221	1.202	1.237	1.266
6500	1.235	1.201	1.22	1.228	1.217	1.265	1.188
7000	1.223	1.217	1.246	1.216	1.258	1.21	1.155
7500	1.223	1.243	1.244	1.237	1.237	1.173	1.164
8000	1.235	1.264	1.235	1.252	1.201	1.168	1.201
8500	1.255	1.267	1.243	1.235	1.183	1.188	1.242
9000	1.275	1.26	1.252	1.213	1.185	1.224	1.244
9500	1.288	1.255	1.248	1.201	1.203	1.256	1.216
10000	1.291	1.259	1.236	1.201	1.232	1.263	1.211
10500	1.287	1.262	1.226	1.213	1.263	1.244	1.256
11000	1.282	1.261	1.222	1.233	1.281	1.23	1.339
11500	1.28	1.256	1.226	1.258	1.28	1.243	1.427
12000	1.282	1.252	1.236	1.283	1.267	1.288	1.491
12500	1.284	1.25	1.251	1.301	1.257	1.352	1.528
13000	1.285	1.251	1.271	1.307	1.263	1.419	1.548
13500	1.284	1.257	1.291	1.303	1.288	1.472	1.558
14000	1.284	1.266	1.311	1.295	1.329	1.509	1.563
14500	1.284	1.278	1.326	1.29	1.377	1.532	1.565
15000	1.286	1.293	1.336	1.293	1.425	1.547	1.567

TABLE-4

Variation of ENTHALPY (J/kg) with Pressure & Temperature

Temp(K)	PRESSURE (atm)						
	100	10	1	0.1	0.01	0.001	0.0001
500	5.051E+05	5.051E+05	5.051E+05	5.051E+05	5.051E+05	5.051E+05	5.051E+05
1000	1.048E+06	1.048E+06	1.048E+06	1.048E+06	1.048E+06	1.048E+06	1.048E+06
1500	1.636E+06	1.636E+06	1.636E+06	1.636E+06	1.636E+06	1.636E+06	1.636E+06
2000	2.250E+06	2.250E+06	2.250E+06	2.256E+06	2.279E+06	2.336E+06	2.531E+06
2500	2.877E+06	2.892E+06	2.935E+06	3.064E+06	3.451E+06	4.420E+06	5.754E+06
3000	3.556E+06	3.659E+06	3.969E+06	4.779E+06	6.139E+06	6.905E+06	7.052E+06
3500	4.360E+06	4.771E+06	5.776E+06	7.112E+06	7.654E+06	7.805E+06	8.066E+06
4000	5.396E+06	6.383E+06	7.738E+06	8.357E+06	8.644E+06	9.287E+06	1.127E+07
4500	6.716E+06	8.124E+06	9.015E+06	9.467E+06	1.051E+07	1.363E+07	2.170E+07
5000	8.223E+06	9.500E+06	1.019E+07	1.142E+07	1.504E+07	2.394E+07	3.367E+07
5500	9.676E+06	1.073E+07	1.197E+07	1.536E+07	2.390E+07	3.406E+07	3.722E+07
6000	1.099E+07	1.224E+07	1.498E+07	2.227E+07	3.323E+07	3.783E+07	3.881E+07
6500	1.235E+07	1.440E+07	1.985E+07	3.071E+07	3.796E+07	3.962E+07	4.091E+07
7000	1.396E+07	1.760E+07	2.652E+07	3.685E+07	4.020E+07	4.157E+07	4.460E+07
7500	1.601E+07	2.204E+07	3.332E+07	4.017E+07	4.206E+07	4.460E+07	5.222E+07
8000	1.874E+07	2.753E+07	3.841E+07	4.232E+07	4.440E+07	4.971E+07	6.578E+07
8500	2.220E+07	3.325E+07	4.169E+07	4.433E+07	4.781E+07	5.818E+07	8.721E+07
9000	2.635E+07	3.820E+07	4.401E+07	4.673E+07	5.293E+07	7.145E+07	1.130E+08
9500	3.097E+07	4.199E+07	4.611E+07	4.987E+07	6.045E+07	8.997E+07	1.340E+08
10000	3.565E+07	4.480E+07	4.833E+07	5.410E+07	7.112E+07	1.113E+08	1.463E+08
10500	3.987E+07	4.713E+07	5.093E+07	5.979E+07	8.522E+07	1.304E+08	1.526E+08
11000	4.347E+07	4.925E+07	5.410E+07	6.728E+07	1.020E+08	1.439E+08	1.562E+08
11500	4.647E+07	5.142E+07	5.799E+07	7.684E+07	1.193E+08	1.521E+08	1.587E+08
12000	4.897E+07	5.380E+07	6.282E+07	8.848E+07	1.344E+08	1.572E+08	1.606E+08
12500	5.123E+07	5.647E+07	6.874E+07	1.017E+08	1.459E+08	1.605E+08	1.624E+08
13000	5.335E+07	5.955E+07	7.581E+07	1.156E+08	1.539E+08	1.630E+08	1.641E+08
13500	5.544E+07	6.308E+07	8.415E+07	1.289E+08	1.595E+08	1.651E+08	1.657E+08
14000	5.762E+07	6.714E+07	9.358E+07	1.405E+08	1.635E+08	1.669E+08	1.673E+08
14500	5.993E+07	7.183E+07	1.040E+08	1.499E+08	1.665E+08	1.687E+08	1.689E+08
15000	6.238E+07	7.715E+07	1.148E+08	1.573E+08	1.689E+08	1.703E+08	1.705E+08

TABLE-5

Variation of Prandtl Number with Pressure & Temperature

Temp(K)	PRESSURE (atm)						
	100	10	1	0.1	0.01	0.001	0.0001
500	0.7380	0.7380	0.7380	0.7380	0.7380	0.7380	0.7380
1000	0.7560	0.7560	0.7560	0.7560	0.7560	0.7560	0.7560
1500	0.7670	0.7670	0.7670	0.7670	0.7670	0.7670	0.7670
2000	0.7730	0.7730	0.7730	0.7660	0.7240	0.6680	0.6140
2500	0.7620	0.7510	0.6960	0.6450	0.6110	0.6540	0.7710
3000	0.7400	0.6800	0.6270	0.6360	0.7400	0.7450	0.7140
3500	0.6780	0.6310	0.6600	0.7440	0.7370	0.6580	0.6060
4000	0.6400	0.6620	0.7620	0.7590	0.6190	0.5800	0.5870
4500	0.6540	0.7430	0.7520	0.6100	0.5780	0.6110	0.7640
5000	0.7020	0.7670	0.6110	0.5810	0.6240	0.7990	0.9930
5500	0.7480	0.6200	0.5830	0.6170	0.7850	0.9890	0.8710
6000	0.7630	0.5920	0.6020	0.7360	0.9690	0.8910	0.4550
6500	0.6100	0.5920	0.6730	0.9060	0.9550	0.4640	0.3920
7000	0.5930	0.6200	0.7960	0.9860	0.8300	0.4040	0.3610
7500	0.5950	0.6880	0.9270	0.9690	0.4240	0.3710	0.3420
8000	0.6200	0.7880	0.9830	0.6480	0.3870	0.3510	0.3220
8500	0.6660	0.8910	0.9430	0.4110	0.3630	0.3550	0.2790
9000	0.7300	0.9610	0.8070	0.3820	0.3480	0.3160	0.2000
9500	0.8060	0.9660	0.4970	0.3640	0.3360	0.2790	0.1140
10000	0.8860	0.8720	0.4290	0.3480	0.3190	0.2160	0.0576
10500	0.9370	0.5320	0.4040	0.3390	0.2950	0.1450	0.0314
11000	0.9550	0.4630	0.3820	0.3270	0.2540	0.0877	0.0213
11500	0.9470	0.4340	0.3690	0.3120	0.2010	0.0524	0.0167
12000	0.9080	0.4120	0.3550	0.2920	0.1460	0.0346	0.0143
12500	0.7280	0.3960	0.3430	0.2630	0.1010	0.0238	0.0129
13000	0.5250	0.3830	0.3330	0.2270	0.0688	0.0190	0.0121
13500	0.4380	0.3690	0.3190	0.1850	0.0470	0.0162	0.0110
14000	0.4210	0.3600	0.3020	0.1440	0.0345	0.0149	0.0108
14500	0.4010	0.3490	0.2770	0.0986	0.0245	0.0130	0.0109
15000	0.3940	0.3410	0.2530	0.0819	0.0129	0.0120	0.0110

TABLE-6

Variation of Thermal Conductivity(W/mK) with Pressure & Temperature

Temp(K)	PRESSURE (atm)						
	100	10	1	0.1	0.01	0.001	0.0001
500	0.0372	0.0372	0.0372	0.0372	0.0372	0.0372	0.0372
1000	0.0624	0.0624	0.0624	0.0624	0.0624	0.0624	0.0624
1500	0.0826	0.0826	0.0826	0.0826	0.0826	0.0826	0.0826
2000	0.0994	0.0994	0.0994	0.1057	0.1233	0.1765	0.337
2500	0.1199	0.1257	0.1545	0.2386	0.4419	0.732	0.5249
3000	0.1496	0.203	0.3369	0.577	0.6339	0.2306	0.1543
3500	0.2219	0.3601	0.5396	0.4527	0.1965	0.2412	0.4241
4000	0.33	0.4834	0.3668	0.1963	0.357	0.741	1.844
4500	0.4203	0.3994	0.2237	0.4333	0.958	2.304	3.981
5000	0.4234	0.2754	0.4538	0.9903	2.294	3.558	1.633
5500	0.3566	0.4218	0.8682	1.987	3.218	1.652	0.5131
6000	0.2927	0.6869	1.545	2.842	1.985	0.6005	0.9311
6500	0.5295	1.103	2.292	2.432	0.8677	0.9357	2.053
7000	0.7702	1.637	2.577	1.366	0.5386	1.798	4.417
7500	1.074	2.124	2.083	1.007	1.467	3.398	8.831
8000	1.444	2.32	1.372	0.6016	2.461	6.104	14.92
8500	1.789	2.096	0.9255	1.764	4.01	10.22	19.53
9000	2.037	1.642	0.6092	2.622	6.372	14.72	17.53
9500	2.09	1.226	1.279	3.9	9.432	17.79	10.55
10000	1.946	0.8026	2.159	5.561	12.78	16.72	5.049
10500	1.684	1.314	2.952	7.602	15.49	12.11	2.315
11000	1.416	1.754	3.969	10	16.27	7.288	1.203
11500	1.184	2.22	5.189	12.33	14.53	4.032	0.7201
12000	1.037	2.805	6.688	14.15	11.17	2.327	0.4956
12500	0.7381	3.436	8.176	14.87	7.69	1.346	0.3993
13000	1.303	4.231	9.761	14.29	5.072	0.9197	0.3656
13500	2.286	5.124	11.19	12.52	3.281	0.7307	0.3357
14000	2.678	6.063	12.24	10.18	2.242	0.6461	0.3713
14500	3.272	7.482	12.92	7.244	1.489	0.579	0.3979
15000	3.624	8.194	12.7	5.891	0.737	0.5648	0.4252

TABLE-7

Variation of Viscosity(Kg m/s) with Pressure & Temperature

Temp(K)	PRESSURE (atm)						
	100	10	1	0.1	0.01	0.001	0.0001
500	2.6710E-05	2.6710E-05	2.6710E-05	2.6710E-05	2.6710E-05	2.6710E-05	2.6710E-05
1000	4.1580E-05	4.1580E-05	4.1580E-05	4.1580E-05	4.1580E-05	4.1580E-05	4.1580E-05
1500	5.2690E-05	5.2690E-05	5.2690E-05	5.2690E-05	5.2690E-05	5.2690E-05	5.2690E-05
2000	6.1920E-05	6.1920E-05	6.1920E-05	6.1920E-05	6.1920E-05	6.1920E-05	6.1920E-05
2500	6.9970E-05	6.9970E-05	6.9970E-05	6.9970E-05	6.9970E-05	6.9970E-05	6.9970E-05
3000	7.7190E-05	7.7190E-05	7.7190E-05	7.7190E-05	7.7190E-05	7.7190E-05	7.7190E-05
3500	8.3810E-05	8.3890E-05	8.4060E-05	8.4310E-05	8.4650E-05	8.4650E-05	8.4730E-05
4000	9.0220E-05	9.0670E-05	9.1390E-05	9.1750E-05	9.1930E-05	9.2110E-05	9.2830E-05
4500	9.6650E-05	9.7800E-05	9.8470E-05	9.8850E-05	9.9330E-05	1.0100E-04	1.0490E-04
5000	1.0330E-04	1.0470E-04	1.0550E-04	1.0630E-04	1.0860E-04	1.0240E-04	1.1940E-04
5500	1.1010E-04	1.1180E-04	1.1260E-04	1.1540E-04	1.2180E-04	1.2850E-04	1.3040E-04
6000	1.1670E-04	1.1860E-04	1.2120E-04	1.2760E-04	1.3650E-04	1.3970E-04	1.3960E-04
6500	1.2420E-04	1.2630E-04	1.3200E-04	1.4360E-04	1.4790E-04	1.4900E-04	1.4730E-04
7000	1.3110E-04	1.3530E-04	1.4540E-04	1.5580E-04	1.5860E-04	1.5690E-04	1.5220E-04
7500	1.3870E-04	1.4660E-04	1.6000E-04	1.6620E-04	1.6680E-04	1.6310E-04	1.5090E-04
8000	1.4740E-04	1.5960E-04	1.7310E-04	1.7680E-04	1.7370E-04	1.6510E-04	1.3820E-04
8500	1.5770E-04	1.7390E-04	1.8440E-04	1.8440E-04	1.7870E-04	1.6060E-04	1.0990E-04
9000	1.6960E-04	1.8740E-04	1.9520E-04	1.9120E-04	1.8000E-04	1.4630E-04	7.0830E-05
9500	1.8280E-04	1.9970E-04	2.0250E-04	1.9620E-04	1.7620E-04	1.2010E-04	3.6760E-05
10000	1.9680E-04	2.1220E-04	2.0890E-04	1.9880E-04	1.6530E-04	8.6030E-05	1.7060E-05
10500	2.1020E-04	2.2180E-04	2.1460E-04	1.9790E-04	1.4570E-04	5.3510E-05	8.1530E-06
11000	2.2270E-04	2.2780E-04	2.1890E-04	1.9230E-04	1.1870E-04	3.0360E-05	4.4020E-06
11500	2.3430E-04	2.3460E-04	2.2110E-04	1.8140E-04	8.8660E-05	1.6770E-05	2.7950E-06
12000	2.4580E-04	2.4120E-04	2.2120E-04	1.6500E-04	6.1410E-05	9.9960E-06	1.9040E-06
12500	2.5550E-04	2.4560E-04	2.1740E-04	1.4270E-04	4.0340E-05	5.8320E-06	1.4580E-06
13000	2.6130E-04	2.4920E-04	2.1060E-04	1.1750E-04	2.6110E-05	3.9670E-06	1.3220E-06
13500	2.6850E-04	2.5140E-04	2.0000E-04	9.2150E-05	1.6850E-05	3.0320E-06	1.1790E-06
14000	2.7440E-04	2.5190E-04	1.8570E-04	7.0020E-05	1.1500E-05	2.5740E-06	1.2010E-06
14500	2.7970E-04	2.4720E-04	1.6420E-04	4.6820E-05	7.3370E-06	2.2710E-06	1.3980E-06
15000	2.8510E-04	2.4650E-04	1.4720E-04	3.7680E-05	2.8440E-06	2.1330E-06	1.4220E-06

TABLE-8

Variation of Compressibility with Pressure & Temperature

Temp(K)	PRESSURE (atm)						
	100	10	1	0.1	0.01	0.001	0.0001
500	1.000	1.000	1.000	1.000	1.000	1.000	1.000
1000	1.000	1.000	1.000	1.000	1.000	1.000	1.000
1500	1.000	1.000	1.000	1.000	1.000	1.000	1.000
2000	1.000	1.000	1.000	1.001	1.002	1.005	1.016
2500	1.000	1.001	1.004	1.011	1.033	1.088	1.163
3000	1.003	1.009	1.026	1.072	1.149	1.192	1.200
3500	1.012	1.035	1.092	1.167	1.197	1.203	1.211
4000	1.033	1.089	1.165	1.198	1.208	1.228	1.287
4500	1.071	1.149	1.196	1.213	1.245	1.337	1.577
5000	1.118	1.186	1.214	1.252	1.359	1.622	1.910
5500	1.159	1.208	1.248	1.348	1.599	1.898	1.990
6000	1.189	1.235	1.316	1.529	1.849	1.983	2.008
6500	1.214	1.279	1.437	1.752	1.961	2.006	2.032
7000	1.243	1.351	1.607	1.904	1.997	2.027	2.088
7500	1.284	1.457	1.778	1.971	2.017	2.067	2.210
8000	1.341	1.590	1.896	2.001	2.044	2.144	2.446
8500	1.418	1.727	1.959	2.023	2.090	2.284	2.826
9000	1.512	1.838	1.993	2.050	2.166	2.510	3.282
9500	1.616	1.914	2.018	2.090	2.286	2.832	3.645
10000	1.718	1.962	2.042	2.149	2.462	3.202	3.843
10500	1.807	1.993	2.071	2.234	2.700	3.526	3.932
11000	1.876	2.018	2.111	2.351	2.983	3.745	3.969
11500	1.927	2.042	2.163	2.505	3.272	3.867	3.985
12000	1.965	2.067	2.232	2.694	3.520	3.931	3.993
12500	1.993	2.098	2.318	2.910	3.700	3.963	3.996
13000	2.017	2.135	2.426	3.135	3.818	3.979	3.998
13500	2.039	2.180	2.553	3.347	3.889	3.988	3.999
14000	2.062	2.233	2.700	3.527	3.932	3.993	3.999
14500	2.086	2.297	2.861	3.667	3.957	3.996	4.000
15000	2.113	2.372	3.028	3.769	3.973	3.997	4.000

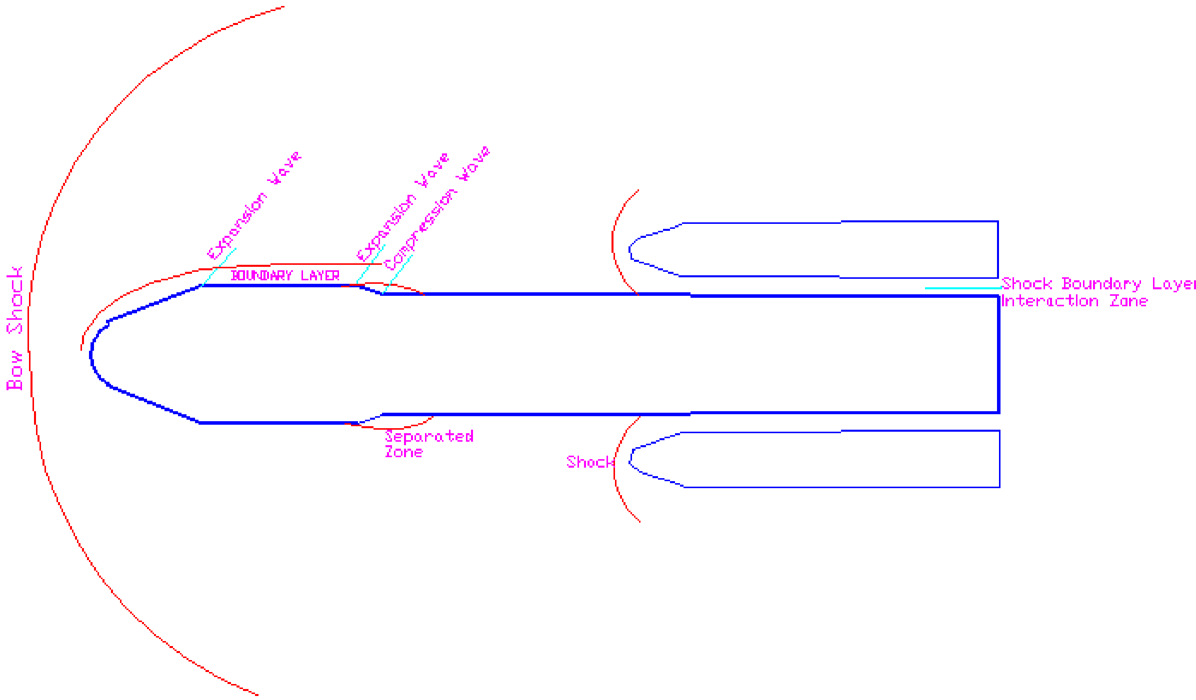

Fig. 1 Flow past a typical launch vehicle

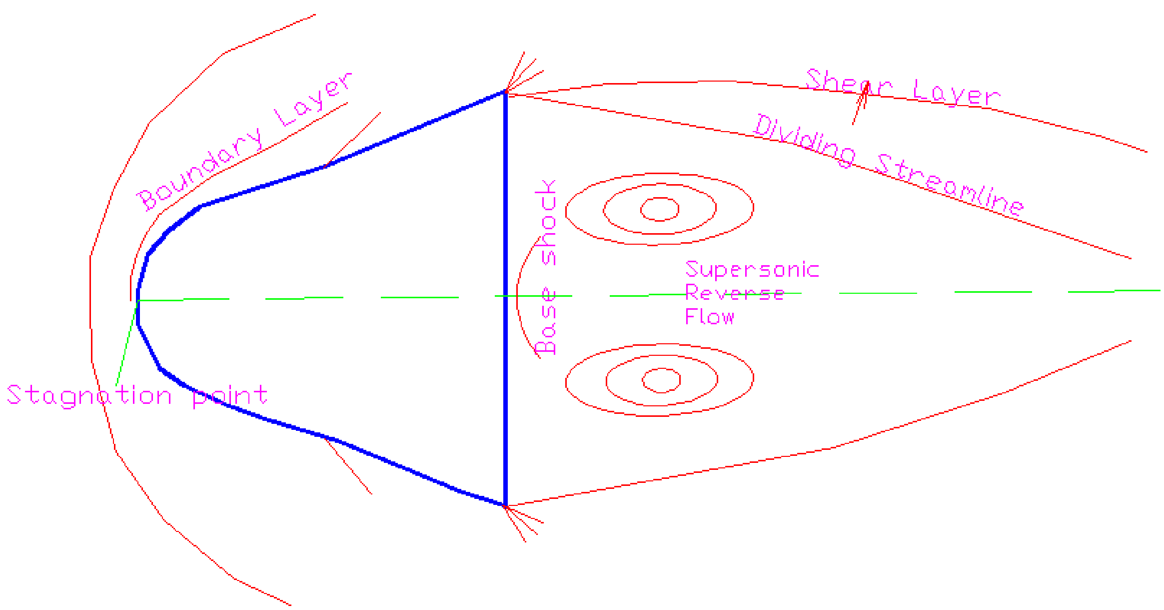

Fig. 2 Flow past a Reentry module

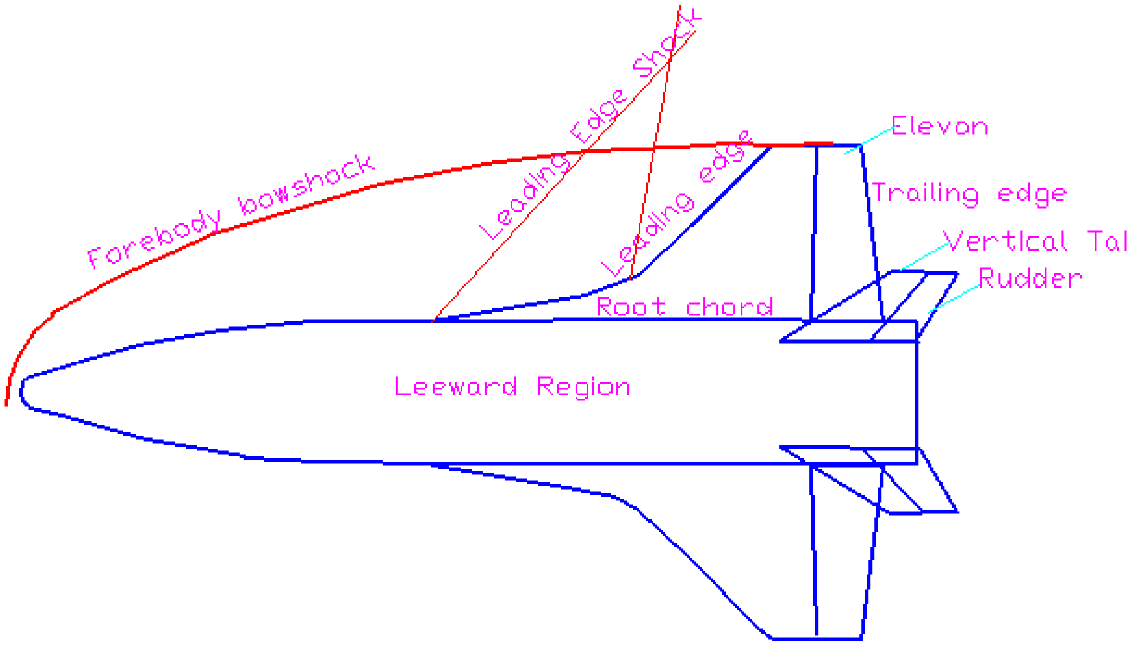

Fig. 3 Flow past a Reusable Launch Vehicle

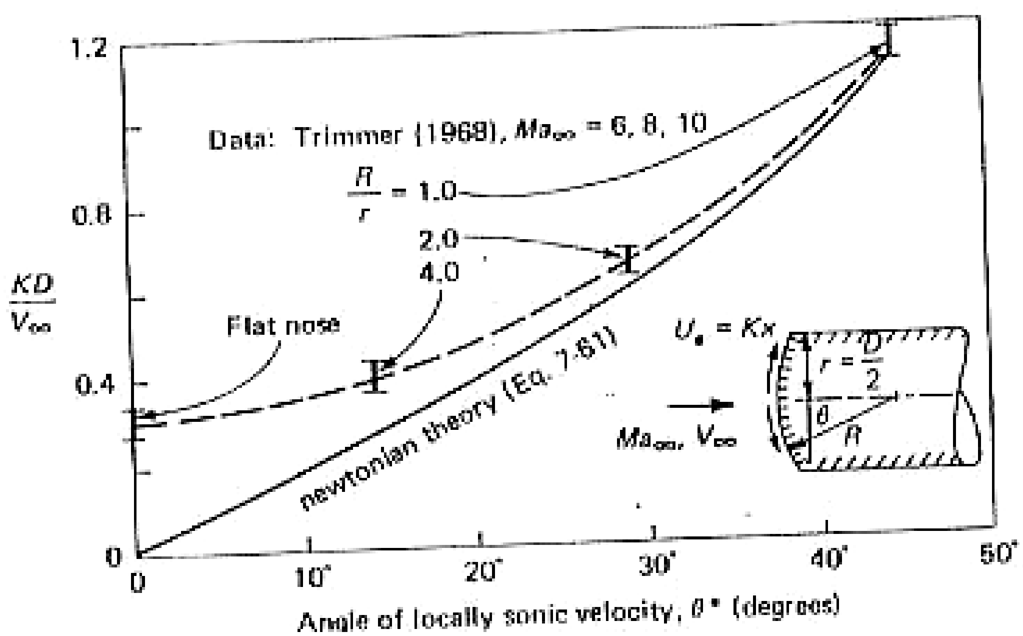

Fig. 4 Comparison of theory and experiment for the stagnation point velocity gradient K on cylinders with spherical noses

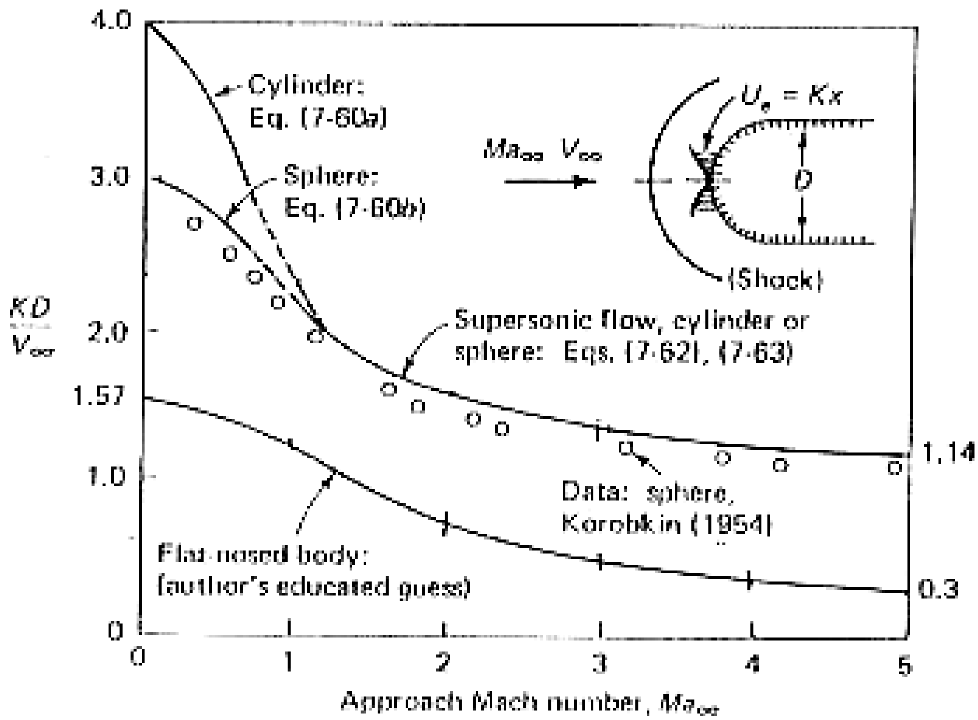

Fig. 5 Theoretical, experimental and estimated stagnation-point velocity gradients on cylinders, spheres and flat noses

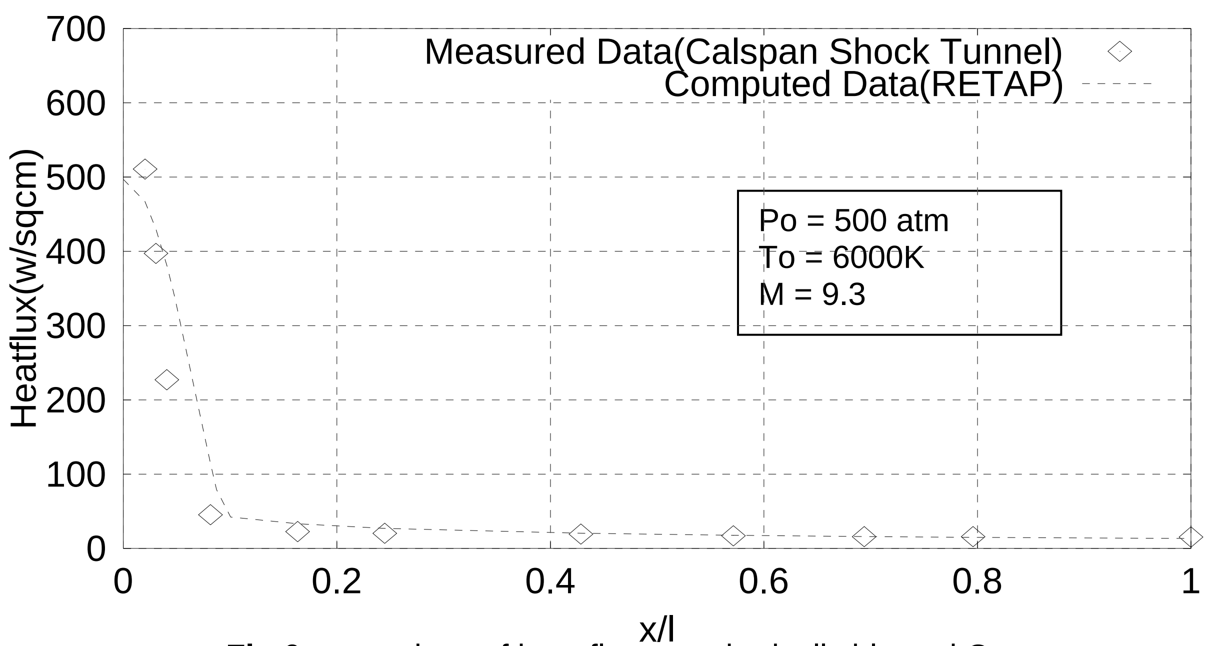

Fig 6 comparison of heat flux on spherically blunted Cone

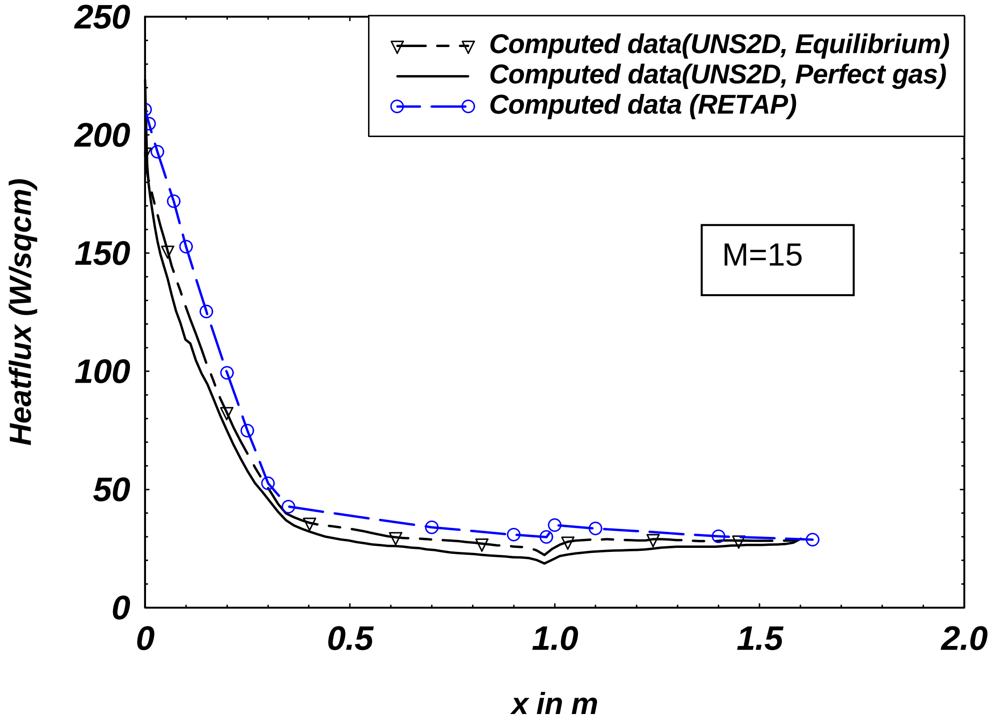

Fig: 7 Comparison of Heat flux between OTAP and UNS2D

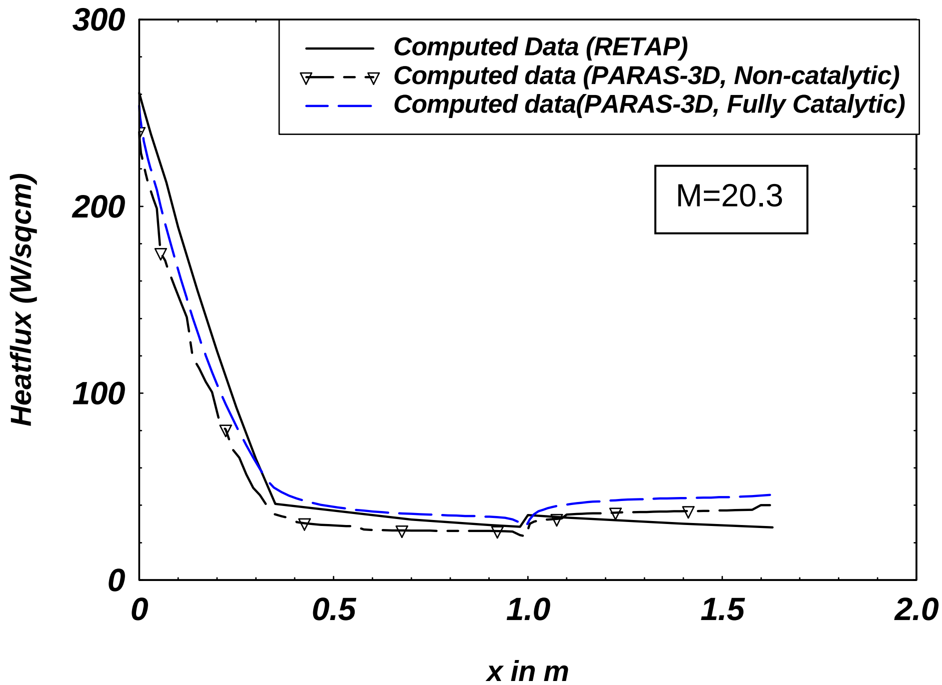

Fig: 8 Comparison of Heat flux between OTAP and PARAS-3D

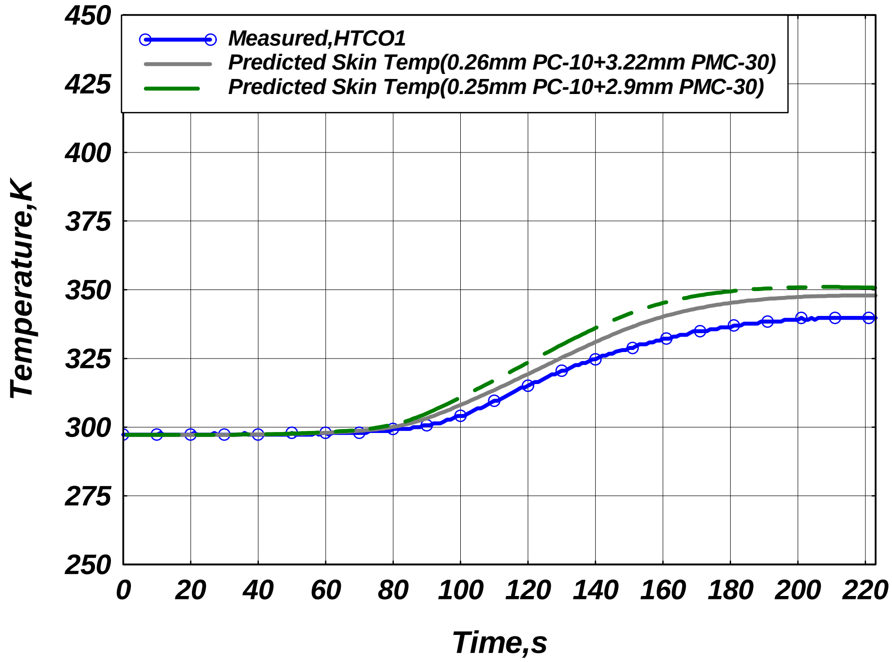

Fig. 9 Comparison between measured and computed temperature histories at cone region for F04 Mission

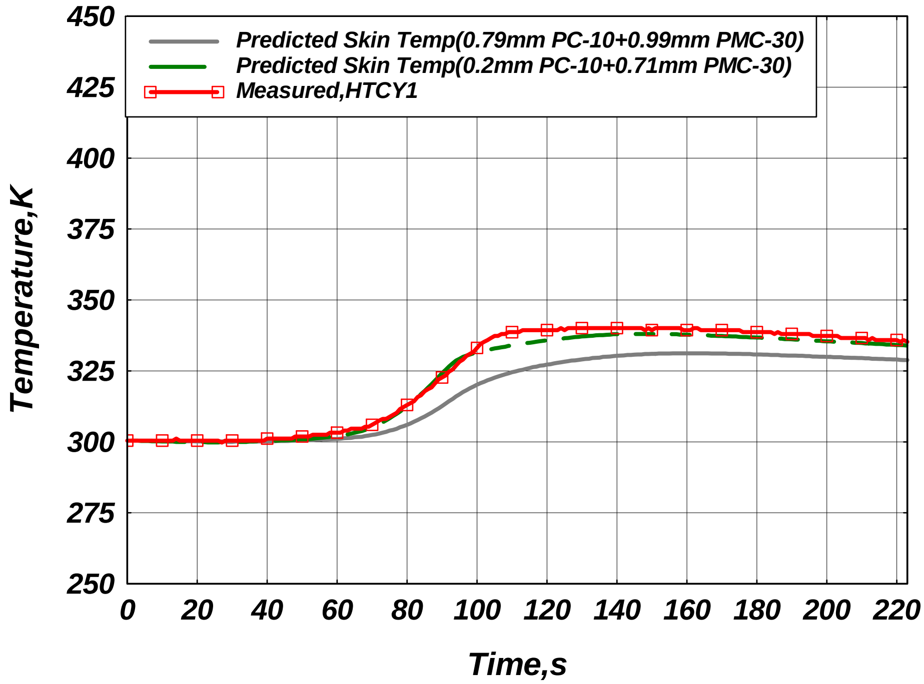

Fig. 10 Comparison between measured and computed temperature histories at cylinder region for F04 Mission

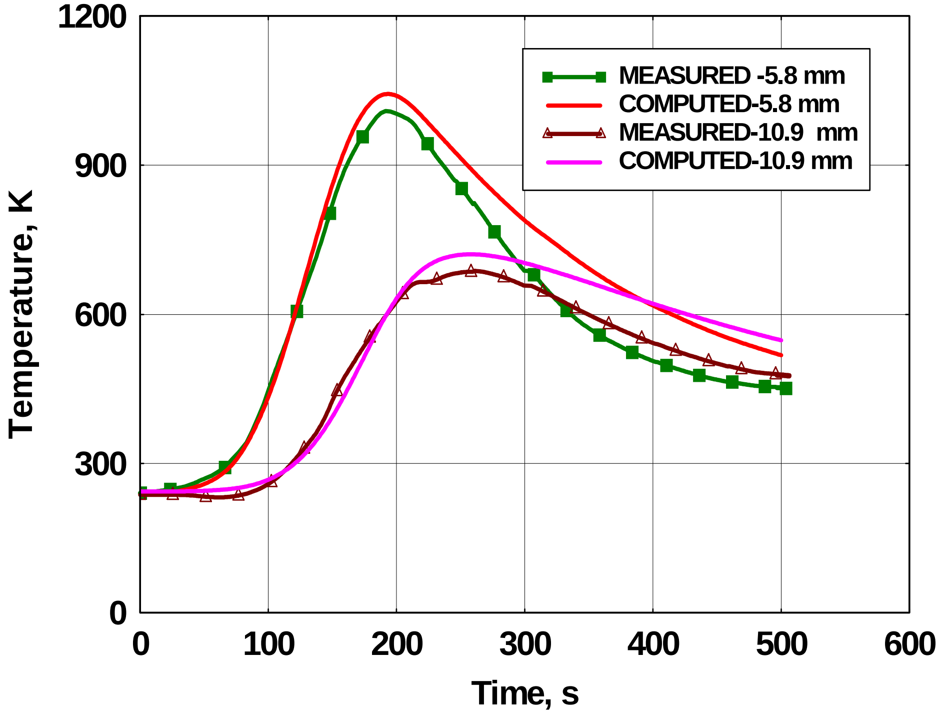

Fig. 11 Thermal Response of Silica Tile in the Conical Region of SRE

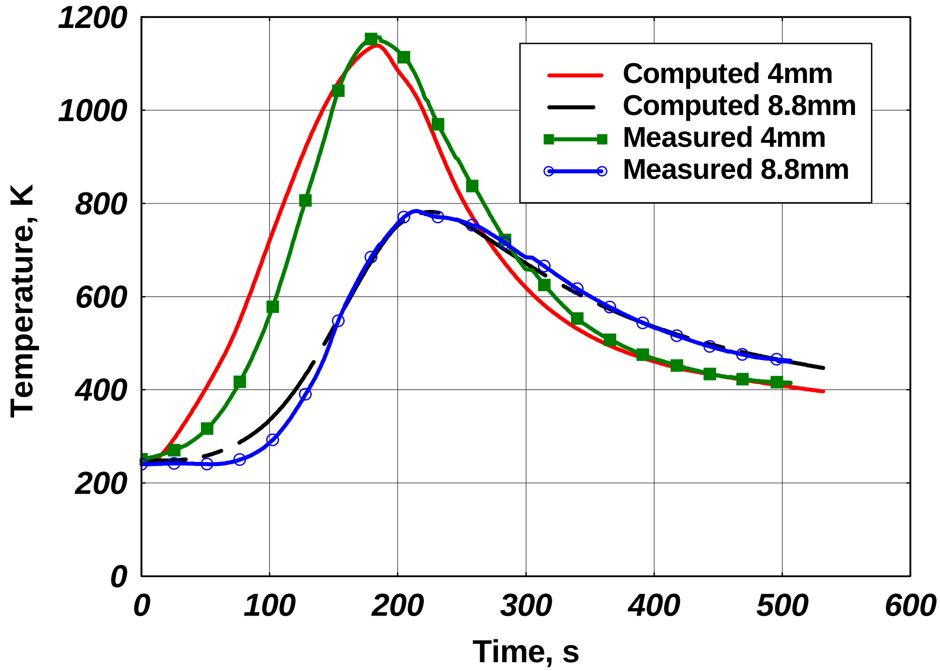

Fig. 12 Thermal Response of Silica Tile in the flare Region of SRE

APPENDIX – A1

Normal Shock Relations for Equilibrium Air

Let p_∞, ρ_∞, u_∞, T_∞, h_∞ denote the free stream values and p_s, ρ_s, u_s, T_s, h_s denote the post-shock values.

We have the following conservative equations for one-dimensional flow.

$$\rho_s u_s = \rho_\infty u_\infty \qquad \text{(Mass) (1)}$$

$$p_s + \rho_s u_s^2 = p_\infty + \rho_\infty u_\infty^2 \qquad \text{(Momentum) (2)}$$

$$h_s + \frac{u_s^2}{2} = h_\infty + \frac{u_\infty^2}{2} \qquad \text{(Energy) (3)}$$

$$h_s = f\left(p_s, T_s\right) \qquad \text{(Enthalpy form) (4)}$$

$$\rho_s = g\left(p_s, T_s\right) \qquad \text{(Equation of state) (5)}$$

Equations (4) and (5) are obtained from Hansen's tables for the properties of equilibrium air. From these five equations, one can solve for the post shock parameters in iterative manner. Post-shock stagnation conditions can be obtained by using the following isentropic relations:

$$p_0 = p_s\left(1 + \frac{\gamma - 1}{2} M_s^2\right)^{\frac{\gamma}{\gamma - 1}}$$

$$T_0 = T_s\left(1 + \frac{\gamma - 1}{2} M_s^2\right)$$

Where γ is evaluated at (p_s,T_s)

Local flow conditions can be obtained from the following equations,

$$p_0 = p_e\left(1 + \frac{\gamma - 1}{2} M_e^2\right)^{\frac{\gamma}{\gamma - 1}}$$

$$T_0 = T_e\left(1 + \frac{\gamma - 1}{2} M_e^2\right)$$

APPENDIX – A2

Inviscid Pressure Distribution

1) Subsonic (potential flow over a sphere)

$$\frac{u}{u_\infty} = \frac{3}{2}\sin\theta$$

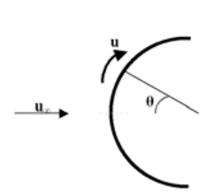

Subsonic (potential flow over a cylinder)

$$\frac{u}{u_\infty} = 2\sin\theta$$

Newtonian pressure distribution for supersonic flow

$$C_p^{'} = C_{po}\sin^2\delta$$

$$C_p = C_{po}\cos^2\theta$$

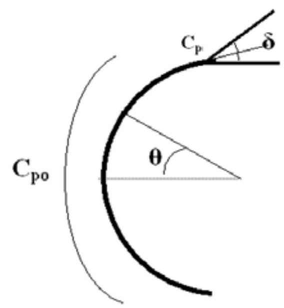

2) Curve fit for cone tables (supersonic flow)

$$\beta = \sqrt{M_\infty^2 - 1}$$

$$\frac{T_e}{T_\infty} = \begin{cases} 1 + 0.35\left(M_\infty \sin\theta\right)^{1.5} & for \quad 0 \le M_\infty \sin\theta \le 1 \\ \left[1 + e^{-(1+1.52 M_\infty \sin\theta)}\right]\left[1 + \dfrac{M_\infty \sin\theta}{2}\right]^2 & for \quad M_\infty \sin\theta \ge 1 \end{cases}$$

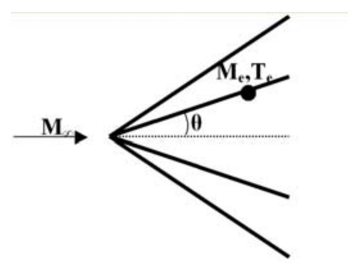

$$\frac{u_e}{u_\infty} = \sin\theta\left[1 - \frac{\sin\theta}{M_\infty}\right]^{1/2}$$

$$Cp = \left(4\sin^2\theta\right)\frac{\left(2.5 + 8\beta\sin\theta\right)}{\left(1 + 16\beta\sin\theta\right)} = \frac{\dfrac{P_e}{P_\infty} - 1}{\gamma M_\infty^2}$$

APPENDIX – A3

Oblique Shock Relations

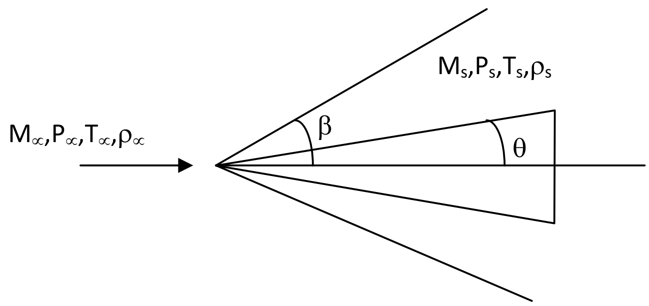

Shock angle β is given in terms of the flow deflection angle θ as follows:

$$\tan\theta = Cot\beta - \frac{2\left[M_\infty{}^2 Sin^2\beta - 1\right]}{M_\infty{}^2\left(\gamma + Cos2\beta\right) + 2}$$

For given Mach number, there is a maximum value of θ_{max} for which the shock is attached. Once β is found from the above relation; other parameters are calculated as follows:

$$\frac{\rho_s}{\rho_\infty} = \frac{(\gamma+1)M_\infty^2 Sin^2\beta}{(\gamma-1)M_\infty^2 Sin^2\beta + 2}$$

$$\frac{p_s - p_\infty}{p_\infty} = \frac{2\gamma}{\gamma+1}\left(M_\infty^2 Sin^2\beta - 1\right)$$

$$\frac{T_s}{T_\infty} = \frac{a_s^2}{a_\infty^2} = 1 + \frac{2(\gamma-1)M_\infty^2 Sin^2\beta - 1}{(\gamma+1)^2 M_\infty^2 Sin^2\beta}\left(\gamma M_\infty^2 Sin^2\beta + 1\right)$$

$$M_s^2 Sin^2(\beta-\theta) = \frac{1 + \frac{(\gamma-1)}{2}M_\infty^2 Sin^2\beta}{\gamma M_\infty^2 Sin^2\beta - \frac{(\gamma-1)}{2}}$$

Oblique Shock Relations (Theory)

(Journal of Aircrafts, Vol. 35, 1998, p. 647)

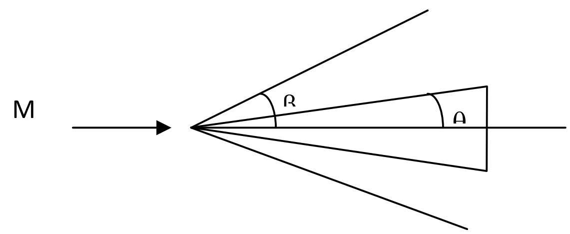

$$\theta = Flow\ deflection\ \ angle$$
$$\beta = Shock\ \ angle$$

$$\frac{\tan(\beta-\theta)}{\tan(\beta)} = \frac{(\gamma-1)M^2 Sin^2\beta + 2}{(\gamma+1)M^2 Sin^2\beta}$$

This can be simplified as

$$\tan\theta = cot\beta - \frac{M^2 sin^2\beta - 1}{1+\left(\frac{(\gamma+1)}{2} - sin^2\beta\right)M^2}$$

This can be written as a cubic in $\tan\beta$ as follows

$$\left(1+\frac{(\gamma-1)}{2}M^2\right)\tan\theta\tan^3\beta - (M^2-1)\tan^2\beta + \left(1+\frac{(\gamma+1)}{2}M^2\right)\tan\theta\tan\beta + 1 = 0$$

This is a cubic in $\tan\beta$. If two of the roots are complex, the shock is detached. If all the roots are real,

$$\tan\beta = \left(\frac{b+9a\tan\mu}{2(1-3ab)} - \frac{d\left(27a^2\tan\mu + 9ab - 2\right)}{6a(1-3ab)}\right)\tan\left(\frac{n\pi}{3} + \frac{1}{3}\tan^{-1}\left(\frac{1}{d}\right)\right)$$

$$n = \begin{cases} 0,\ Weak\ shock \\ 1,\ Strong\ \ shock \\ -1,\ Physically\ meaningless\ solution \end{cases}$$

$$\mu = Mach\ \ wave\ angle \qquad \left(sin\mu = \frac{1}{M}\right)$$

$$a = \left(\frac{\gamma-1}{2} + \frac{\gamma+1}{2}\tan^2\mu\right)\tan\theta$$

$$b = \left(\frac{\gamma+1}{2} + \frac{\gamma+3}{2}\tan^2\mu\right)\tan\theta$$

$$d = \sqrt{\frac{4(1-3ab)^3}{(27a^2c+9ab-2)^2} - 1}$$

Only weak shock solution is taken.

Oblique Shock Relations (SHWAVE PROGRAM)

$$c = \frac{2}{(\gamma - 1)\tan\theta\left(M^2 + \frac{2}{(\gamma-1)}\right)} \qquad \theta = Flow\,deflection\,angle \qquad \beta = Shock angle$$

$$b = \frac{\left(\frac{\gamma+1}{\gamma-1}M^2 + \frac{2}{(\gamma-1)}\right)}{\left(M^2 + \frac{2}{(\gamma-1)}\right)}$$

$$a = c(1 - M^2)$$

$$p = -\frac{a^2}{3} + b$$

$$q = \frac{2a^3}{27} - \frac{ab}{3} + c$$

$$s = \left(\frac{p}{3}\right)^3 + \left(\frac{q}{2}\right)^2$$

$\underline{s < 0}$

$$b_1 = \sqrt{\frac{-p}{3}}$$

$$a_1 = \frac{-s}{2b_1^3} \qquad \phi = Cos^{-1}(a_1)$$

$$Z_1 = 2b_1 Cos\left(\frac{\phi}{3}\right) - \frac{a}{3}$$

$$Z_2 = -2b_1 Cos\left(\frac{\phi}{3} + \frac{\pi}{3}\right) - \frac{a}{3}$$

$$Z_3 = -2b_1 Cos\left(\frac{\phi}{3} - \frac{\pi}{3}\right) - \frac{a}{3}$$

$$if\ (\max(Z_1, Z_2, Z_3) < 0, \quad \text{Shock is detached}$$

$$\beta = \tan^{-1}(Z_2) \quad ; \quad M_2 = \frac{\sqrt{\frac{(\gamma-1)x^2 + 2}{2\gamma x^2 - (\gamma-1)}}}{Sin(\beta - \theta)} \quad ; \quad x = MSin(\beta)$$

$\underline{s = 0}$

$$a_1 = \sqrt{s} - \frac{q}{2}$$

$$b_1 = -\sqrt{s} - \frac{q}{2}$$

$$z_1 = (a_1 b_1)^{\frac{1}{3}} - \frac{a}{3}$$

$$\beta = \tan^{-1}(Z_1) \qquad if \quad (\beta < 0), \ \text{Shock is detached}$$

APPENDIX – A4

Fay and Riddel Formula for Stagnation Point Heat Transfer

$$q = k\left(\Pr\right)^{-0.6}\left(\rho_w \mu_w\right)^{0.1}\left(\rho_o \mu_o\right)^{0.4}\left(H_o - H_w\right)\sqrt{\left.\frac{du}{ds}\right|_{s=0}}\left\{1 + (Le^{\beta} - 1)\frac{H_D}{H_o}\right\}$$

where $k = \begin{cases} 0.763 \text{ for axisymmetric flow} \\ 0.57 \text{ for two-dimensional flow} \end{cases}$

$\alpha = \left.\dfrac{du}{ds}\right|_{s=0}$ is the velocity gradient at the stagnation point.

$$\beta = \begin{cases} 0.52 \text{ for frozen flow} \\ 0.63 \text{ for equilibrium flow} \end{cases}$$

Le is Lewis number (usually taken as 1.4)

H_D is the energy of dissociation

H_o is the Total stagnation enthalpy

Velocity gradient for various nose shapes

- ✓ **Thick infinite plate or flat-headed cylinder (D thickness or diameter)**

$$\frac{\alpha D}{u_\infty} = \begin{cases} 1.57 - 0.408M & (M < 2.5) \\ 0.5 - 0.08(M - 2.5)) & (2.5 < M < 5) \\ 0.3 & (M > 5) \end{cases}$$

- ✓ **Cylinder**

$$\frac{\alpha D}{u_\infty} = 4 - 1.664M^2 \quad (M < 1)$$

$$\alpha = \frac{1}{r_N}\sqrt{\frac{2(P_O - P_\infty)}{\rho_O}} \quad (M > 1)$$

- ✓ **Sphere**

$$\frac{\alpha D}{u_\infty} = 3 - 0.756M^2 \quad (M < 1)$$

$$\alpha = \frac{1}{r_N}\sqrt{\frac{2(P_O - P_\infty)}{\rho_O}} \quad (M > 1)$$

Energy of Dissociation

$$H_D = 0.79\sqrt{\frac{F_{N_2}}{1+F_{N_2}}}.E_{N_2} + 0.21\sqrt{\frac{F_{O_2}}{1+F_{O_2}}}.E_{O_2} \quad (\text{cal/gm})$$

where $E_{N_2} = 4183$ and $E_{O_2} = 7023$

$$F_{N_2} = \frac{P_{N_2}}{P}.\frac{T}{T_{N_2}}e^{\left(-\frac{T_{N_2}}{T}\right)}$$

$$F_{O_2} = \frac{P_{O_2}}{P}.\frac{T}{T_{O_2}}e^{\left(-\frac{T_{O_2}}{T}\right)}$$

$$P_{N_2} = 4.5\,\text{x}10^7$$

$$P_{O_2} = 2.3\,\text{x}10^7$$

$$T_{N_2} = 113200$$

$$T_{O_2} = 59000$$

P is pressure in atmospheres and T is the temperature in Kelvin.

Equilibrium Air Composition

Partition functions are given as

$$\ell n\,Q(O) = \frac{5}{2}\ell nT + 0.5 + \ell n\left(5 + 3e^{\frac{-228}{T}} + e^{\frac{-326}{T}} + 5e^{\frac{-22800}{T}} + e^{\frac{-48600}{T}}\right) - \ell n\,P$$

$$\ell n\,Q(N) = \frac{5}{2}\ell nT + 0.3 + \ell n\left(4 + 10e^{\frac{-27700}{T}} + 6e^{\frac{-41500}{T}}\right) - \ell n\,P$$

$$\ell n\,Q(O^+) = \frac{5}{2}\ell nT + 0.5 + \ell n\left(4 + 10e^{\frac{-38600}{T}} + 6e^{\frac{-58200}{T}}\right) - \ell n\,P$$

$$\ell n\,Q(N^+) = \frac{5}{2}\ell nT + 0.3 + \ell n\left(1 + 3e^{\frac{-70.6}{T}} + 5e^{\frac{-188.9}{T}} + 5e^{\frac{-22000}{T}} + e^{\frac{-47000}{T}} + 5e^{\frac{-679000}{T}}\right) - \ell n\,P$$

$$\ell n\,Q(e^-) = \frac{5}{2}\ell nT - 14.24 - \ell n\,P$$

$$\ell n\,Q(N_2) = \frac{7}{2}\ell nT - 0.42 - \ell n\left(1 - e^{\frac{-3390}{T}}\right) - \ell n\,P$$

$$\ell n\,Q(O_2) = \frac{7}{2}\ell nT + 0.11 - \ell n\left(1 - e^{\frac{-2270}{T}}\right) - \ell n\left(3 + 2e^{\frac{-11390}{T}} + e^{\frac{-18990}{T}}\right) - \ell n\,P$$

Equilibrium constants for the 4 major reactions are given by

$$\ell nKp_1\left(O_2 \rightarrow 2O\right) = -\frac{59000}{T} + 2\ell nQ_p(O) - \ell nQ_p(O_2)$$
$$\ell nKp_2\left(N_2 \rightarrow 2N\right) = -\frac{113200}{T} + 2\ell nQ_p(N) - \ell nQ_p(N_2)$$

$$\ell nKp\left(O \rightarrow O^+ + \overline{e}\right) = -\frac{158000}{T} + \ell nQ_p(O^+) - \ell nQ_p(\overline{e}) - \ell nQ_p(O)$$

$$\ell nKp\left(N \rightarrow N^+ + \overline{e}\right) = -\frac{168000}{T} + \ell nQ_p(N^+) - \ell nQ_p(\overline{e}) - \ell nQ_p(N)$$

$$Q_p = pQ$$

$$\varepsilon_1 = \frac{-0.8 + \left[0.64 + 0.8(1 + 4p/kp_1)\right]^{1/2}}{2\left(1 + \dfrac{4p}{kp_1}\right)}$$

$$\varepsilon_2 = \frac{-0.4 + \left[0.16 + 3.84(1 + 4p/kp_2)\right]^{1/2}}{2\left(1 + \dfrac{4p}{kp_2}\right)}$$

where $Kp_3 = 0.2\,Kp\left(O \rightarrow O^+ + \overline{e}\right) + 0.8\,Kp\left(N \rightarrow N^+ + \overline{e}\right)$

The component mole fractions are given by

$$X\left(O_2\right) = \frac{0.2 - \varepsilon_1}{Z}$$

$$X\left(N_2\right) = \frac{0.8 - \varepsilon_2}{Z}$$

$$X\left(O\right) = \frac{2\varepsilon_1 - 0.4\varepsilon_3}{Z}$$

$$X\left(N\right) = \frac{2\varepsilon_2 - 1.6\varepsilon_3}{Z}$$

$X\left(O^+ + N^+\right) = X\left(\overline{e}\right) = \dfrac{2\varepsilon_3}{Z}$ where Z is the compressibility factor given by

$$Z = 1 + \varepsilon_1 + \varepsilon_2 + \varepsilon_3$$

APPENDIX – A5

Lees Formula for Laminar Heat Transfer in the Stagnation Region

$$\frac{q}{q_0}=\frac{2\theta Sin\theta\left\{\left[1-\frac{1}{\gamma M_\infty^2}\right]Cos^2\theta+\frac{1}{\gamma M_\infty^2}\right\}}{\left[D(\theta)\right]^{1/2}} \qquad \left[0\le\theta\le\left(D-\theta_c\right)\right]$$

$$D(\theta)=\left(1-\frac{1}{\gamma M_\infty^2}\right)\left(\theta^2-\frac{\theta Sin4\theta}{2}+\frac{1-Cos4\theta}{8}\right)+\frac{4}{\gamma M_\infty^2}\left(\theta^2-\theta Sin2\theta+\frac{1-Cos2\theta}{8}\right)$$

q_0 is the heat transfer at the stagnation point.

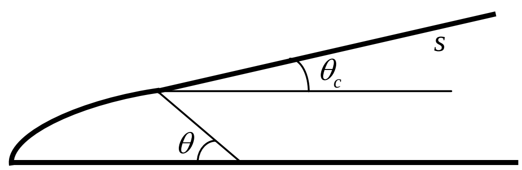

In the case of spherically blunted cone, heat transfer on the cone is given by

$$\frac{q}{q_0}=A\left(\theta_c\right)+\frac{\left(\frac{s^{'}}{r_N}\right)}{\left[B(\theta_c)+\left(\frac{s^{'}}{r_N}\right)^2\right]^{1/2}}$$

Where $\frac{s^{'}}{r_N}=\cot\theta_c+\left[\frac{s}{r_N}-\left(\frac{\pi}{2}-\theta_c\right)\right]$

$$A\left(\theta_c\right)=\frac{\sqrt{3}}{2}\left[\left(1-\frac{1}{\gamma M_\infty^2}\right)\sin^2\theta_c+\frac{1}{\gamma M_\infty^2}\right]^{1/2}\sqrt{\left(\frac{\pi}{2}-\theta_c\right)}$$

$$B\left(\theta_c\right)=\frac{3/16}{\sin^2\theta_c\left\{\left[1-\frac{1}{\gamma M_\infty^2}\right]\sin^2\theta_c+\frac{1}{\gamma M_\infty^2}\right\}}\left[\frac{D\left(\theta\right)}{\theta}\right]-\cot^3\theta_c$$

$$where\ \theta=\frac{\pi}{2}-\theta_c$$

APPENDIX – A6

Van Driest Formula for Turbulent Flow over Flat Plate

C_f is given by the following equation

$$\frac{0.242}{A\sqrt{C_f \frac{T_w}{T_e}}}\left(\sin^{-1}\alpha+\sin^{-1}\delta\right)=0.41+\log_{10}\left(\mathrm{Re}_s . C_f\right)-\left(n+0.5\right)\log_{10}\left(\frac{T_w}{T_e}\right)$$

where $\alpha=\dfrac{2A^2-B}{(B^2+4A^2)^{1/2}}$ and $\delta=\dfrac{B}{(B^2+4A^2)^{1/2}}$

Re is the local Reynolds number and C_f is the local skin friction coefficient.

$$A^2=\frac{\left(\gamma-1\right)M_e^2}{2\left(\frac{T_w}{T_e}\right)}; \quad B=\frac{1+\frac{\gamma-1}{2}M_e^2}{\left(\frac{T_w}{T_e}\right)}-1$$

Stanton Number $C_h=\dfrac{C_f}{2}.\gamma_{af}$ where γ_{af} is the Reynolds analogy factor.

Heat flux, $\quad q=C_h\rho_e u_e\left(H_{rec}-H_w\right)$

$H_{rec}=h_e+rec\left(\dfrac{u_e^2}{2}\right)$ where rec is the recovery factor.

$$\gamma_{af}=\mathrm{Pr}_t\left[1+5\sqrt{\frac{c_f}{2}}\left\{\frac{(1-\mathrm{Pr}_t)}{5K}\left(\frac{\pi^2}{6}+\frac{3}{2}-\frac{3}{2}\mathrm{Pr}_t\right)+\left(\frac{\mathrm{Pr}}{\mathrm{Pr}_t}-1\right)+\ln\left(\frac{1}{6}+\frac{5}{6}\frac{\mathrm{Pr}}{\mathrm{Pr}_t}\right)\right\}\right]$$

$$\mathrm{rec}=\mathrm{Pr_t}\left[\begin{array}{l}1+\frac{2}{\mathrm{k}}\sqrt{\frac{\mathrm{C_f}}{2}}(1-\mathrm{Pr_t})\left\{\frac{\pi^2}{6}+1.5(1-\mathrm{Pr_t})\right\}+\\ 12.5\mathrm{C_f}\left\{\frac{\mathrm{Pr}}{\mathrm{Pr_t}}-1+2\ln\left(\frac{1}{6}+\frac{5}{6}\frac{\mathrm{Pr}}{\mathrm{Pr_t}}\right)+\ln(6)\ln\left(\frac{1}{8}+\frac{7}{8}\frac{\mathrm{Pr}}{\mathrm{Pr_t}}\right)-\ln(6)\ln\left(\frac{3}{4}+\frac{1}{4}\frac{\mathrm{Pr}}{\mathrm{Pr_t}}\right)\right\}\end{array}\right]$$

where k is the Karman mixing length constant (k =0.4)

n is the exponent in viscosity law (n = 0.707)

$\mathrm{Pr_t}$ is the turbulent Prandtl number ($\mathrm{Pr_t}$ = 0.86)

Van Driest Formula for Laminar Flow over Flat Plate

$$C_f = \frac{F_1 + F_2\left(\frac{T_W}{T_e}\right)}{\sqrt{\mathrm{Re}_S}}$$

where $F_1 = 0.416594 + \left(0.246733\text{E-2}\right)\mathrm{M_e} - \left(0.817489\text{E-3}\right)\mathrm{M_e^2} + \left(0.2734033\text{E-4}\right)\mathrm{M_e^3}$

$$F_2 = -\left(0.134671\text{E-1}\right) + \left(0.2635807\text{Ee-3}\right)\mathrm{M_e} + \left(0.581944\text{E-4}\right)\mathrm{M_e^2} - \left(0.2173257\text{E-5}\right)\mathrm{M_e^3}$$

Reynolds Analogy Factor, $\gamma_{af} = \mathrm{Pr}^{2/3}$

Recovery Factor, $r_e = \mathrm{Pr}^{1/2}$

APPENDIX – A7

Eckert Formula for Flat plate Flow

h_e - Static enthalpy

T_e - Total enthalpy

Recovery factor, $rec = \begin{cases} \Pr^{\frac{1}{2}}, & laminar\ flow \\ \Pr^{\frac{1}{3}}, & turbulent\ flow \end{cases}$

$$H_{rec} = h_e + rec.\frac{u_e^2}{2}$$

From H_{rec}, T_{rec} is calculated using Newton-Raphson iteration and Hansen's tables.

$$T_{rec}^{n} = T_{rec}^{n-1} + \frac{\left(H_{rec} - H_r\right)^{n-1}}{Cp^{n-1}}$$

Starting from an initial value of $T_{rec} = T_e + \left(1 + \frac{\gamma - 1}{2} M_e^2 .rec\right)$

The reference temperature T^* is calculated iteratively by matching reference enthalpy H^*, using Hansen's tables. The reference enthalpy H^* is calculated as

$$H^* = 0.5\left(H_w - H_e\right) + 0.22\left(H_{rec} - H_e\right)$$

The local Reynold's number is calculated using the reference temperature T^*, for evaluating ρ^* and μ^*.

$$\mathrm{Re}^* = \frac{\rho^* u_e r}{\mu^*}$$

The local skin friction coefficient C_f is computed using Re^*.

$$C_f = \begin{cases} \dfrac{0.664}{\left(\mathrm{Re}^*\right)^{\frac{1}{2}}}, & laminar\ flow \\ \dfrac{0.37}{\left(\log_{10} \mathrm{Re}^*\right)^{2.584}}, & turbulent\ flow \end{cases}$$

Stanton number is now computed using Reynold's analogy factor as follows

$$C_h = \begin{cases} \dfrac{C_f}{2} Pr^{\frac{1}{2}}, & laminar\ flow \\ \dfrac{C_f}{2} Pr^{\frac{2}{3}}, & turbulent\ flow \end{cases}$$

Heat flux is estimated as $\dot{q} = \rho_e u_e \left(H_{rec} - H_W\right) = \rho_e u_e c_h \left(T_{rec} - T_W\right)$

Heat transfer coefficient $= \rho_e u_e c_h$

APPENDIX – A8

Chen and Thyson Formula for Boundary Layer Transition

Intermittency factor is given by

$$\gamma_{tr} = 1 - \exp\left[-G\ r_o(x_{tr}) \int_{x_{tr}}^{x} \frac{dx}{r_O} \int_{x_{tr}}^{x} \frac{dx}{u_e} \right] \qquad (1)$$

where r_o is the local body radius, x_{tr} is the location of the onset of transition

G is a spot formation rate parameter defined by $G = \frac{3}{C^2}\left(\frac{Ue^2}{\upsilon e^2}\right)\mathrm{Re}_{tr}^{-1.34}$

where $C = 4.86 M_e^{1.92} + 60$

Re_{tr} is the transition Reynolds number, $\upsilon_e = \frac{\mu_e}{\rho_e}$

In the case of cylindrical and flat plate flow, r_o and u_e are constants.

Equation (1) becomes $$\gamma_{tr} = 1 - \exp\left[\frac{-3}{C^2} (\mathrm{Re}_x - \mathrm{Re}_{tr})^2\ \mathrm{Re}_{tr}^{-1.34} \right]$$

In the case of conical and wedge flow, $r_o = x \tan\alpha$ and u_e is constant.

Equation (1) becomes $$\gamma_{tr} = 1 - \exp\left[\frac{-3}{C^2} \left(\mathrm{Re}_x - \mathrm{Re}_{tr}\right)\ \ln\frac{\mathrm{Re}_x}{\mathrm{Re}_{tr}}\ \mathrm{Re}_{tr}^{-0.34} \right]$$

$$C_f = \gamma_{tr} C_{f_{turb}} + (1 - \gamma_{tr}) C_{f_{lam}}$$

APPENDIX – A9

Heat Transfer along the Windward Generator of a Swept Infinite Cylinder: (Beckwith & Gallagher)

Turbulent Flow

$$\frac{hD}{k}=\left[\frac{u_\infty D}{\gamma_\infty}\right]^{0.8} Pr^{1/3}\left[0.0228\frac{\mu_w}{\mu_o}\frac{T_\infty}{T_w}\frac{P_s}{P_\infty}\right]^{0.8} Sin^{0.6}\lambda\left\{0.13032\frac{\mu_o}{\mu_\infty}Cos\lambda\frac{D}{V_N}.\left(\frac{dV_N}{dx}\right)_s\right\}^{0.2}$$

Where D is the diameter of the cylinder

λ is the sweep back angle

u_∞ is the free stream velocity

$V_N = u\sin\lambda$

k is conductivity of air

$\frac{dV_N}{dx}$ is the velocity gradient at stagnation point

$$\dot{q}=h(T_{rec}-T_w)$$

Laminar Flow (Modified Fay and Riddel formula)

$$\frac{R_D}{k}=0.5\left(2\frac{Re_\infty}{M_\infty}\frac{\mu_s}{\mu_\infty}\right)^{\frac{1}{2}}\left[\frac{2}{\gamma}\frac{T_\infty}{T_s}\frac{p_s}{p_\infty}\left(\frac{p_s}{p_\infty}-1\right)\right]^{\frac{1}{4}}(\cos\lambda)^{1.1}$$

$$\dot{q}=0.57Pr^{-0.6}\left(\rho_w\mu_w\right)^{0.1}\left(\rho_o\mu_o\right)^{0.4}(H_o-H_w)\sqrt{\left(\frac{dV_N}{dx}\right)_s}*0.7071(Cos\lambda)^{1.15}$$

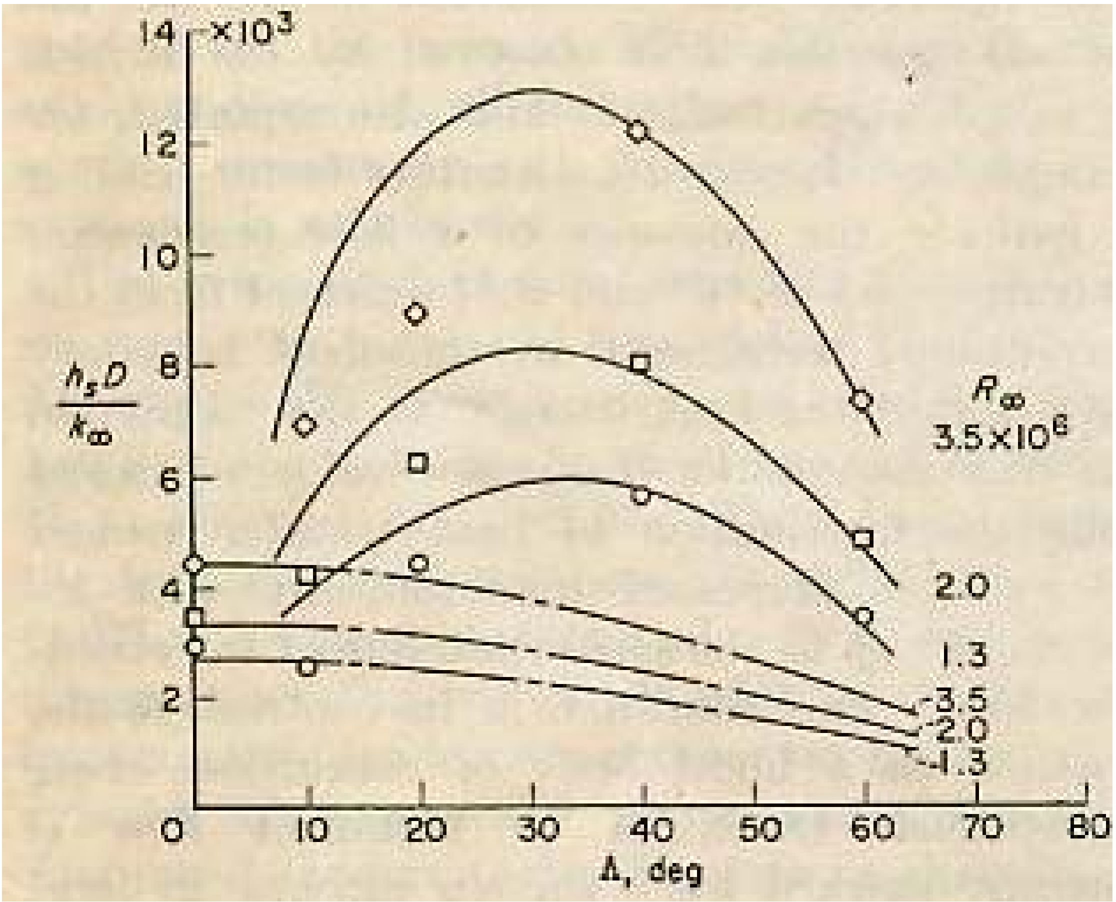
14
×10³
12
10
8
6
4
2
$h_s D / k_\infty$
R_∞
3.5×10⁶
2.0
1.3
3.5
2.0
1.3
0
10
20
30
40
50
60
70
80
Λ, deg

APPENDIX – A10

Free Molecular and Transitional Flows

Flow regimes are characterized based on Knudsen number (Kn), which is defined as

$$K_n = \frac{\lambda}{c}$$

Where λ is the mean free path and c is a characteristic length (usually the body dimension or boundary layer thickness δ).

$$\lambda = \frac{\mu}{\rho}\sqrt{\frac{\pi}{2RT}}$$

Based on boundary layer thickness, $K_n = \sqrt{\frac{\pi r}{2}}\frac{M}{\sqrt{\text{Re}}}$, for Re >> 1.

Based on body length, $K_n = \sqrt{\frac{\pi r}{2}\frac{M}{\text{Re}}}$, for Re < 1.

Knudsen Number	Flow Type
Kn < 0.01	Continuum
0.01 < Kn < 1	Slip
1 < Kn < 10	Transition
Kn > 10	Free molecular

Heat transfer in the intermediate regime is given as

$$q_{tran} = pq_{free} + (1-p)q_{continuum}$$
$$where\ p = \frac{Kn}{1+Kn}$$

Free molecular heat transfer is given by

$$q_{tran} = \alpha\rho RT_{\infty}\sqrt{\frac{RT_{\infty}}{2\pi}}\left\{\left(s^2 + \frac{r}{r-1} - \frac{r+1}{2(r-1)}\frac{T_w}{T_{\infty}}\right) + \left(e^{-(s\sin\theta)^2} + \sqrt{\pi}s\sin\theta\left(1+erf\ s\sin\theta\right)\right) - \frac{1}{2}e^{-(s\sin\theta)^2}\right\}$$

Where α is the accommodation coefficient

S is the speed ratio, $s = \frac{\mu_{\infty}}{\sqrt{2RT_{\infty}}}$

θ is the flow angle of incidence

APPENDIX – A11

Free Convection and Radiation inside the air gap of a Multilayer Insulation system

In the air layer, all the three modes of heat transfer take place and for solving the multilayer conduction equation an equivalent conductivity can be estimated.

Two dimensional free convection between Parallel Plates (with length L and gap h)

Rayleigh number,

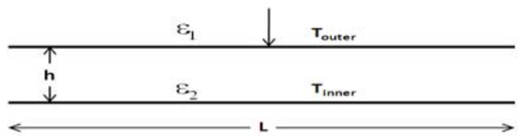

$$Ra = \frac{g\beta\left(T_{outer} - T_{inner}\right)}{\upsilon\left(\frac{k}{\rho c_p}\right)},$$

$$\upsilon = \frac{\mu}{\rho} \text{ and } \beta = \frac{2}{\left(T_{outer} + T_{inner}\right)}$$

$$\overline{Ra} = Ra.\frac{h}{L}$$

$$C_l = \frac{4}{3} * 0.48\left(\frac{\Pr}{\Pr + 0.861}\right)^{\frac{1}{4}}$$

Define $C_3 = 12 * 0.919 * C_l^{\frac{1}{4}}$

Then the heat transfer parameter (Nusselt number) is given by

$$Nu = C_l\left(\overline{Ra}\right)^{\frac{1}{4}} S$$

and heat transfer coefficient is given as

$$h_c = \frac{Nu.k}{h}$$

where $S = \sum_{n=1}^{\infty} C_3^{n-1}\left(-1\right)^{n-1}\frac{3}{\left(4n-1\right)\left(n-1\right)!}$

Free convection heat flux between the plates,

$$q_c = h_c\left(T_{outer} - T_{inner}\right)$$

Axissymetric Free Convection in the Annular Region between Two Co-axial Infinite Cylinders (with gap h)

Rayleigh number,

$$Ra = \frac{g\beta\left(T_{outer} - T_{inner}\right)h^3}{\upsilon\left(\frac{k}{\rho c_p}\right)}$$

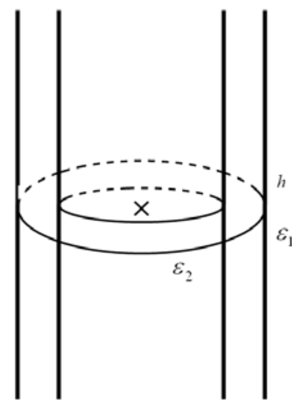

$$\overline{Ra} = \frac{Ra \ln\left(\frac{D_{outer}}{D_{inner}}\right)^4}{h^3\upsilon\left(D_{outer}^{-0.6} + D_{inner}^{-0.6}\right)^5}$$

$$K_{eff} = 0.386\left(\frac{\Pr}{\Pr + 0.861}\right)^{\frac{1}{4}}\left(\overline{Ra}\right)^{\frac{1}{4}}$$

$$h_c = \frac{2k\,k_{eff}}{\ln\left(\frac{D_{outer}}{D_{inner}}\right)D_{inner}} \qquad Nu = \frac{2h\,h_c}{k}$$

Free convection heat flux between the cylinders is

$$q_c = h_c\left(T_{outer} - T_{inner}\right)$$

<u>Radiative heat flux between the two surfaces</u>

Define $F = \sqrt{1 + \left(\frac{L}{R}\right)^2} - \frac{h}{L}$ $\quad (for\ 2D)$

$F = \frac{D_{inner}}{D_{outer}}$ $\quad (for\ axis-symmetric)$

Define $\varepsilon_{equivalent} = \dfrac{1}{\dfrac{(1-\varepsilon_1)}{\varepsilon_1} + \dfrac{(1-\varepsilon_2)}{\varepsilon_2} + \dfrac{1}{F}}$

Radiative flux $q_{rad} = \sigma\varepsilon_{eq}\left(T_{outer}^4 - T_{inner}^4\right)$

APPENDIX – A12

Input Variables

1. TITLE : 80 CHARACTERS

2. INPUT CARDS:

Card 1	Card 2	Card 3	Card 4	Card 5	Card 6	Card 7	Card 8	Card 9	Card 10
ITIPR	**ITERPR**	**IMACH**	**IKHS**	**NCOMP**	**IAXISM**	**IPAR**	**ICART**	**ITHIN**	**KELVIN**

Card 11	Card 12	Card 13	Card 14	Card 15	Card 16	Card 17	Card 18	Card 19	Card 20
ITABLE	**ISHK**	**INV**	**IGM**	**IT**	**ICOND**	**ITRAN**	**IAIR**	**IFRC**	**IRAD**

ITIPR	= 0	No detailed print
	= 1	Detailed print at each time step
	= N	Detailed print after n time step
ITERPR	= 0	No detailed print during iteration
	= 1	Detailed print during iteration interval mentioned in the following line
IMACH	= 0	Mach no history is read in trajectory
	= 1	Velocity history is read in trajectory
IKHS	= 0	Aerodynamic heating is computed
	= 1	Heat flux history is given as input
NCOMP		No of geometrical component on the body
IAXISM	= 0	The flow is two dimensional
	= 1	The flow is axi-symmetric
IPAR	= 0	No perturbation on nominal values of various parameters
	= 1	Perturbation ratios given in variable **PAR** read afterwards
ICART	= 0	Cartesian coordinate for conduction analysis
	= 1	Cylindrical coordinate for conduction analysis
	= 2	Spherical coordinate for conduction analysis
ITHIN	= 0	Thin layer option not used in phase change studies
	= 1	Thin layer option used in phase change studies
KELVIN	= 0	Temperature values in table in Kelvin
	= 1	Temperature values in table in Celsius

ITABLE	= 0	Tables of output parameters not required
	= 1	Tables with parameters after each time steps
	= N	Tables with parameters after n time steps
ISHK	= 0	No shock is considered ahead of body
	= 1	Ideal shock ahead of body
	= 2	Real shock ahead of body
INV		Parameters used for inviscid flow field selection
IGM		Parameter used for defining geometry for stagnation point computation
(Case 1: IAXISM=0)		
IGM	= 1	Thick infinite flat plate (for IAXISM=0)
	= 2	Cylinder in cross flow with no sweep
	= 3	Cylinder in cross flow with sweep, laminar
	= 4	Cylinder in cross flow with sweep, turbulent
(Case 2: IAXISM=1)		
IGM	= 1	Flat heat cylinder
	= 2	Cone frustum
	= 3	Sphere
IT	= 0	Flow can be laminar transitional or turbulent
	= 1	Flow is considered turbulent for low value of Reynolds No: also
ICOND	= 0	Thermal response analysis required
	= 1	Coldwall heatflux
ITRAN	= 1	Transition from laminar to turbulent flow is based on Reynolds No. using wetted length
	= 2	Transition from laminar to turbulent flow is based on Reynolds No. using momentum thickness
IAIR	= 0	If no air layer is considered
	= N	If the nth layer is air layer considered
IFRC	= 1	Free convection to be considered at inner surface
	= 0	Free convection not to be considered at inner surface
IRAD	= 1	Radiation to be considered at the inner surface
	= 0	Radiation from the inner surface not to be considered

3. PRINT COMMANDS: TITER1,TITER2(READ IF ITERPR=1)

TITER1	Time for starting iteration print
TITER2	Time for stopping iteration print

4. INPUT FOR CYLINDRICAL & SPHERICAL COORDINATE SYSTEM: RRT (READ IF ICART ≠ 0)

RRT	Outer radius for cylindrical and spherical co-ordinate systems

5. LIMITING LENGTHS FOR THIN LAYER OPTIONS: X1THIN,X2THIN(READ IF ITHIN#0)

X1THIN	Thickness of first layer less than which thin layer options are exercised
X2THIN	Thickness of second layer less than which thin layer options are exercised

6. INPUTS FOR AIR COLUMNS / GAPS: EL,EH,E1,E2(READ IF IAIR#0)

EL	Length of air column if ICART = 0 Outer radius of air column if ICART ≠ 0
EH	Gap of air column if ICART = 0 Inner radius of air column if ICART ≠ 0
E1	Emissivity of outer surface close to air column
E2	Emissivity of inner surface close to air column

7. FREE CONVECTION PARAMETERS: AL,TAMB(READ IF IFRC # 0)

AL	Length of body participating in free convection heat transfer
TAMB	Ambient temperature

8. AMBIENT TEMPERATURE: TAMB(READ IF IRAD #0)

TAMB	AMBIENT TEMPERATURE

9. GEOMETRY DESCRIPTION VARIABLES: (RR(I), EPS(I), RL(I), I=1, NCOMP)

RR(I)	Rounding radius of each geometrical component in the vehicle configuration
EPS(I)	Body angle of each geometrical
RL(I)	Length of each geometrical component in the vehicle configuration

10. FLOW PARAMETERS: RETR,RETS,ALAMDA,ALFA,QRAD,QINS,RC,GIN

RETR	Transition Reynolds No:
RETS	Reynolds no at the station where transition is initiated
ALAMDA	Sweep angle
ALFA	Total angle of attack
QRAD	Radiative heat input
QINS	Heat generated inside

RC	Typical body dimension for computation of Knudsen number
GIN	Initial value of gas constant (GIN = 1.2 for reentry trajectories)

11. NUMBER OF TRAJECTORY POINTS: NT

NT	Total number of trajectory points

12. TRAJECTORY DATA: TIMM(I),ALT(I),AMACH(I),ALPHA(I),I=1,NT)

TIMM(I)	Time values in trajectory input
ALT(I)	Altitude values in trajectory input
AMACH(I)	Mach no values in trajectory input
ALPHA(I)	Angle of attack values in trajectory input

13. INITIAL CONDITION & CONVERGENCE CRITERIA: TW1,MPD,MCD,TOL1,TOL2

TW1	Initial temperature
MPD	Initial rate at which charring is taking place
MCD	Initial rate at which ablation is taking place
TOL1	Upper limit error for convergence in temperature
TOL2	Upper limit for convergence in charring or ablation rates

14. TIME OF START & STOP: TIN, TFINAL

TIN	Initial time for starting computation
TFIN	Final time for stopping computation

15. NUMBER OF STEPS IN COMPUTATION INTERVAL: NDT

NDT	No of steps in changing computation interval

16. TIME ARRAY FOR COMPUTATION INTERVAL CHANGE: TIA(I),DTA(I),I=1,NDT

TIA (I)	Time array for computation interval change
DTA (I)	Time step array for computation interval change

17. DEFINE MATERIAL, THICKNESS & OPTIMIZATION CONTROL PARAMETERS: NLAYER,(L(I),I=1,NLAYER),LAYOPT,MOPT(M(I)=1,NLAYER),X,(X3(I),I=1,NLAYER), OPTW,TOLOPT,DXOPT,ISUBLM

NLAYER	No of material layer analysis
L(I)	No of computational steps in in each layer
LAYOPT	Index of the interface node where temperature constraint is to be maintained
MOPT	Index of the material layer whose thickness is to be optimized

		for meeting the temperature constraint
M(I)		Material index of each layer as given in material file
X		Axial distance from nose tip
X3(I)		Material thickness for each layer
OPTW		Temperature constraint
TOLOPT		Tolerance for convergence on temperature constraint
DXOPT		Initial trial variation in the thickness of layer to be optimized
ISUBLM	= 0	First layer is not subliming type
	= 1	First layer is subliming type

18. AUGMENTATION / PERTURBATION PARAMETERS: PAR(I),I=1,16 (READ IF IPAR=1)

PAR (I)	Perturbation values for various parameters
PAR (1)	Heat transfer co-efficient
PAR (2)	Emissivity
PAR (3)	Char layer density
PAR (4)	Char layer specific heat
PAR (5)	Char layer conductivity
PAR (6)	Virgin layer density
PAR (7)	Virgin layer specific heat
PAR (8)	Virgin layer conductivity
PAR (9)	Third layer density
PAR (10)	Third layer specific heat
PAR (11)	Third layer conductivity
PAR (12)	Specific heat of pyrolysis gas
PAR (13)	Ablation temperature
PAR (14)	Heat of ablation
PAR (15)	Pyrolysis temperature
PAR (16)	Heat of pyrolysis

APPENDIX – A13

List of Subroutines

Main Program

The main program reads various inputs (like the body geometry, trajectory, inviscid data and material properties) and various options. Various control parameters for output are also read along with other inputs. The input variables are printed after reading for verification. The variable types and dimensions are defined in the main program. For a specified location on body, the main program calls other subroutines in a sequence and stores the results like heat flux and temperature distribution. Based on these inputs, writing of the various parameters is also carried out in this module. Storing of all relevant variables for further processing as well as writing in tables is carried out in this module. The flow chart of the software code is given in **Fig. 18**. Following are the subroutines used in the software package.

BODY

This subroutine computes the local radius, surface distance and body angle for the given axial location by using the vehicle geometry

ATMOS

For the altitude under consideration, this subroutine computes the free stream properties of temperature, pressure, density and sonic speed.

MATPRO

From a material library, this subroutine reads the temperature dependent properties of thermal conductivity, specific heat, density (with phase change) and emissivity and later during the computation computes the properties at all nodal points. It also reads the char-ablation properties for applicable cases.

SHOCK

This subroutine computes the flow properties after a normal shock by solving one-dimensional conservation of mass, momentum and energy, numerically using Hansen's tables.

SHWAVE

For a given free stream Mach number and flow deflection angle, this subroutine computes the flow properties after an oblique shock.

INVSCD

This subroutine computes the local flow properties (pressure, temperature and Mach number) at the boundary layer edge, from the post shock conditions using isentropic relations based on the local pressure or Mach number (either read as input or using build in routines).

GASPRO

The air properties for ideal gas and real gas options are evaluated in this subroutine. For computation of equilibrium air properties, the subroutine calls Subroutine HANSEN

HANSEN

Subroutine HANSEN evaluates thermo-dynamic and transport properties of air at given temperature and pressure. There are two options built in the program. The properties are interpolated from a given table.

STAGPT

This subroutine computes the stagnation point heat flux using the method of Fay and Riddell and the stagnation line heat flux using Beckwith and Gallagher formula.

HEATSR

The heat flux in the stagnation region is computed in this subroutine using the method of Lees where the stagnation point heat flux is also used.

AEROHT

This subroutine computes the heat flux at a location on the aft-body. For laminar as well as transitional turbulent flows, using Van Driest or Eckert Formulas [5].

FREEMOL

The heat flux in the free-molecular regime is computed in this subroutine using standard correlations available.

TRANMOL

The heat in the transition regime (transition from free-molecular to continuum) is computed here using both free-molecular and continuum heat flux values.

TEMP1D

This subroutine computes the tri-diagonal matrix of finite difference equations generated using fully implicit scheme.

SURM1D

This subroutine computes the mass loss and the surface movement in case of ablation or melting and charring rate and interface movement in case of pyrolysis.

SOURCE

Any heat generation or dissipation is introduced in the finite difference equation here.

BOUNDS

The finite difference equations are modified in this subroutine to take care of surface boundary conditions.

BOUNDI

The finite difference equations are modified in this subroutine to take care of inside boundary conditions.

GAUSS

This subroutine computes the nodal temperatures from the finite difference equations using the tri-diagonal matrix solution procedure.

LINEA

This is a subroutine for linear interpolation from a given table.

APPENDIX – A14

Output Variables

1. **TI,ALTI,EMINF,ALFA,TINF,ROINF,PINF,EME,TE,ROE,UE,PE,REY,CF,CH,TAW,EKS,P,QFM, QCONT,IFL,ITRN,RATIO,TO,GO,DYNP,CFL,CFT,HOI**

TI		Current time
ALTI		Altitude at time T1
EMINF		Mach Number at time T1
ALFA		Angle of attack
TINF		Free stream temperature
ROINF		Free stream density
PINF		Free stream pressure
EME		Mach No. at boundary layer edge
TE		Temperature at boundary layer edge
ROE		Density at boundary layer edge
UE		Velocity at boundary layer edge
PE		Pressure at boundary layer edge
Rey		Reyonlds No: at boundary layer edge
CF		Skin friction coefficient
CH		Stanton number
TAW		Adiabatic wall temperature
EKS		Knudsen number
P		Intermittency factor between free molecular and continuum heat flux
QFM		Free molecular heat flux
QCONT		Continuum heat flux
IFL		Parameter showing condition of flow
IFL	= 0	Continuum flow
	= 1	Transition flow
	= 2	Free molecular flow
ITRN		Parameter showing number of iterations
RATIO		Ratio of heat flux on specific location on sphere to heat flux at stagnation point
TO		Total temperature
GO		Ratio of specific heats of gases at temperature TO
DYNP		Dynamic pressure
CFL		Laminar skin friction coefficient
CFT		Turbulent skin friction coefficient
HOI		Total enthalpy

2. H,TW,QAAERO,QNET,QQW,MPD,MCD,X1,X2

H	Heat transfer coefficient
TW	Wall temperature
QAERO	Heat flux due to aerodynamic heating
QNET	Net heat flux
QQW	Instrument heating
MPD	Rate of char formation
MCD	Rate of char ablation
X1	Current thickness of first layer
X2	Current thickness of second layer

3. (T(I), I = IFIRST, ILAST)

T(I)	Temperature at different nodal points

APPENDIX – A15

Sample of Input File

RLV AERODYNAMIC HEATING FOR HEX MISSION NOSECAP (RLV PROJECT) upper bound

```
ITI,  ITER,  IMA,  IKHS, NCO, IAX, IPA, ICAR, ITHN,  KEL,  ITAB,   ISHK,   INV,   IGM,  IT,   CON, ITR,   IAI,   IFR,   IRA,  IAL
100    0     1      0      2    1    1      0      0      0      10      2      4      3    0    1     1     0      0      0     1
0.125 14.0 0.418 0.0 0.0 6.5
0.50E+06 0.0 0.0 0.0 0.0 0.0 0.125 1.4
1037
0              15.188        0              0              0              0
10             488.249       108.401        0.3134         -1.5737          6.5671
20             2227.821      249.331        0.7338         -0.4844          29.3963
30             4944.63       327.958        0.9898         -0.4524          38.4456
-----          -----         -----             -----       -----
-----          -----         -----                         -----             -----
1000           875.735       126.367        0.3668         6.6442           8.5994
1010           632.031       125.071        0.3621         6.6374           8.6242
1020           391.307       123.742        0.3574         6.6305           8.6353
1036           10.515        121.725        0.3502         6.6217           8.6524

313.0 2*0.0 1.0 0.0
0.0 1.0 1036.0 13*0.0 1036.0
1 50 0 0 41 0.0 0.003 1033.0 1.0 0.0001 0
0.0  15*0.0
```

Sample of Output File

RLV AERODYNAMIC HEATING FOR HEX MISSION NOSECAP (RLV PROJECT) upper bound

ITIPR=10 ITERPR= 0 IMACH= 1 IKHS= 0 NCOMP= 2 IAXISM= 1 IPAR= 1 ICART= 0 ITHIN= 0 KELVIN= 0 ITABLE=10

ISHK= 2 INV= 4 IGM= 3 IT= 0 ICOND= 1 ITRAN= 1 IAIR= 0 IFRC= 0IRAD= 0 IALFA= 1

RADIUS,ANGLE + LENGTH FOR EACH PART IS

0.125000 14.000000 0.418000

0.000000 0.000000 6.500000

RETR= 0.50000E+06 RETS= 0.00000E+00 ALAMDA= 0.00 ALFA= 0.00 QAB= 0.000 QINS= 0.000 RC= 0.125

TRAJECTORY DATA

TIME

0.00E+00 1.00E+00 2.00E+00 3.00E+00 4.00E+00 5.00E+00 6.00E+00 7.00E+00 8.00E+00 9.00E+00

1.03E+03 1.03E+03 1.03E+03 1.03E+03 1.03E+03 1.04E+03 1.04E+03

ALT

1.52E-02 1.65E-02 2.61E-02 4.54E-02 7.46E-02 1.14E-01 1.65E-01 2.28E-01 3.02E-01 3.89E-01

```
--------------------------------------------------------------------------------------------------------------------------------------------------------------------------------
   1.53E-01  1.29E-01  1.05E-01  8.17E-02  5.80E-02   3.42E-02    1.05E-02
```

MACH.NO

```
  0.00E+00  5.46E+00  1.48E+01  2.47E+01  3.50E+01   4.59E+01   5.72E+01   6.91E+01   8.16E+01     9.47E+01
--------------------------------------------------------------------------------------------------------------------------------------------------------------------------------
--------------------------------------------------------------------------------------------------------------------------------------------------------------------------------
  1.22E+02  1.22E+02  1.22E+02  1.22E+02  1.22E+02   1.22E+02   1.22E+02
```

ANGLE OF ATTACK

```
  0.00E+00 -4.20E-03 -1.09E-02 -2.01E-02 -7.40E-01 -2.46E+00  -3.46E+00  -3.65E+00  -3.00E+00    -2.24E+00
--------------------------------------------------------------------------------------------------------------------------------------------------------------------------------
--------------------------------------------------------------------------------------------------------------------------------------------------------------------------------
  6.62E+00  6.62E+00  6.62E+00  6.62E+00  6.62E+00   6.62E+00   6.62E+00
         0         1      1036         0         0          0          0          0          0            0          0          0          0
         0         0         0      1036
   PAR-        0          0          0          0          0          0          0          0          0
   0           0          0          0          0          0          0
```

LOCATION= 0.000000

THICKNESS 0.003000

NLAYER= 1 L= 50

TWI= 313.00 MPD= 0.00000 MCD= 0.00000 TOL1= 1.00000 TOL2= 0.00000

LAYER NO. 1 INCONEL 71

	TEMP	CONDUCTIVITY	TEMP	SP.HEAT	TEMP	DENSITY	TEMP	EMISSIVITY
+	0.300000E+03	0.262700E-02						
+			0.300000E+03	0.920000E-01				
+					0.293000E+03	0.822000E+04		
+							273.000000	0.500000
+	0.373000E+03	0.284300E-02						
+			0.513000E+03	0.979000E-01				
+					0.973000E+03	0.822000E+04		
+							973.000000	0.500000
+	0.473000E+03	0.324900E-02						
+			0.605000E+03	0.109400E+00				
+	0.573000E+03	0.363100E-02						
+			0.715000E+03	0.123300E+00				

```
+    0.973000E+03   0.520800E-02
+                                                0.833000E+03   0.138100E+00
+    0.107300E+04   0.561400E-02
+                                                0.901000E+03   0.146400E+00
+    0.157300E+04   0.752500E-02
+                                                0.103500E+04   0.163200E+00
+                                                0.113800E+04   0.175000E+00
  TA=  5000.00   TP=  5000.00   HA=    1.00   HP=    2.00   RAW110=    3.00   RAW10=    4.00   RAW20=    5.00
```

INITIAL TEMP DISTRIBUTION

```
      313.0    313.0    313.0    313.0    313.0    313.0    313.0    313.0    313.0    313.0    313.0
      313.0    313.0    313.0    313.0    313.0    313.0    313.0    313.0    313.0    313.0    313.0
      313.0    313.0    313.0    313.0    313.0    313.0    313.0    313.0    313.0    313.0    313.0
      313.0    313.0    313.0    313.0    313.0    313.0    313.0    313.0    313.0    313.0    313.0
      313.0    313.0    313.0    313.0    313.0    313.0    313.0
-----------------------------------------------------------------------------------------------------------------------------------
  X=   0.00000E+00    Y=   0.00000E+00    S=   0.00000E+00    THET=   0.90000E+02    IC=   0
```

***** ITERATION CONVERGED *****

TIME=0.1000E+01 ALT= 0.017 M8= 0.016 U8= 5.5 T8=300.6 R8=0.1167E+01 P8=0.1027E+05 REN=0.3449E+06 TAUW=0.1738E+02 HO= 72.15

EME= 0.00 TE= 300.61 UE=0.00000E+00 PE=0.10273E+05 ROE=0.11676E+01 REY=0.00000E+00 CFL=0.00000E+00 CFT=0.00000E+00 CF=0.00000E+00

EKS=0.53995E-06 P= 0.000 QFM=0.00000E+00 QCONT=-.83906E-01 IFL= 0 ITR= 0 0 0 0 0 0 0 0 0 0 RATIO= 0.000

GE= 0.000 CH=0.00000E+00 TAW= 0.0 TRCR=0.00000E+00 REZ=0.00000E+00 FACT=0.000 IBL= 0 ELN=0.00000E+00 HD=0.00000E+00 FRF=0.99933E+00

TIME=0.1036E+04 ALT= 0.011 M8= 0.350 U8= 121.7 T8=300.6 R8=0.1168E+01 P8=0.1028E+05 REN=0.7699E+07 TAUW=0.8654E+04 HO= 73.92

EME= 0.00 TE= 308.01 UE=0.00000E+00 PE=0.11188E+05 ROE=0.12410E+01 REY=0.00000E+00 CFL=0.00000E+00 CFT=0.00000E+00 CF=0.00000E+00

EKS=0.53968E-06 P= 0.000 QFM=0.00000E+00 QCONT=-.16462E+00 IFL= 0 ITR= 1 50 50 50 50 50 50 50 50 1 RATIO= 0.000

GE= 0.000 CH=0.14013E-44 TAW= 0.0 TRCR=0.00000E+00 REZ=0.00000E+00 FACT=0.000 IBL= 0 ELN=0.00000E+00 HD=0.00000E+00 FRF=0.99673E+00

TIME=0.1400E+01 ALT= 0.000 M8=****** U8= 0.0 T8= 0.0 R8=0.0000E+00 P8=0.0000E+00 REN=0.1400E+01 TAUW=0.1228E-35 HO= 1.00

EME=

PO=0.1119E+05 TO= 308.0 CPP= 0.000000

H= 0.32989E-01 TW= 313.0 QAERO= -0.165 QNETT= -0.230 QQW= 0.00000 MPD= 0.00000 MCD= 0.00000 X1=0.300000E-02 X2=0.000000E+00

RLV AERODYNAMIC HEATING FOR HEX MISSION NOSECAP (RLV PROJECT) upper bound

0.3000E-02

LOCATION= 0.000000

THICKNESS 0.003000

TIME	ALT	M8	ME	REY.NO	TAUW	H	TAW	QAERO	QNET	TEMP.DISTRIBUTION		
10	0.49	0.31	0	6.61E+06	6.57E+03	1.22E-02	303.6	-0.119	-0.147	3	313	313
80	28.55	5.61	0	2.62E+06	3.32E+04	2.50E-02	1535.5	30.479	30.452	3	313	313
83	31.16	6.22	0	1.93E+06	2.79E+04	2.39E-02	1847.7	36.22	36.192	3	313	313
100	45.54	5.86	0	2.26E+05	3.60E+03	8.81E-03	1864.5	13.325	13.298	3	313	313
180	77.31	6.26	0	3.60E+03	3.98E+01	8.72E-04	1547	1.074	1.046	0	313	313
200	76.38	6.24	0	4.18E+03	4.66E+01	7.04E-04	1551.8	0.877	0.85	35	313	313
280	42.06	5.28	0	3.23E+05	4.56E+03	6.91E-03	1571.5	8.812	8.784	35	313	313
288	38.4	5	0	5.16E+05	6.62E+03	8.51E-03	1408.6	9.418	9.39	32.7	313	313
300	35.37	4.45	0	7.23E+05	7.90E+03	9.80E-03	1150.1	8.217	8.19	27.3	313	313
400	32.89	2.66	0	6.31E+05	3.98E+03	6.97E-03	569	1.788	1.761	16.2	313	313
500	20.53	1.88	0	3.46E+06	1.29E+04	1.22E-02	355.5	0.519	0.491	5	313	313
600	13.57	0.81	0	4.71E+06	7.70E+03	9.23E-03	238.8	-0.686	-0.713	6.9	313	313
700	9.25	0.63	0	5.69E+06	8.88E+03	1.08E-02	265.6	-0.514	-0.542	6.2	313	313
800	6.23	0.49	0	5.99E+06	8.07E+03	1.14E-02	278.7	-0.39	-0.418	6.7	313	313
900	3.43	0.42	0	6.76E+06	8.41E+03	1.25E-02	291.4	-0.269	-0.297	6.7	313	313
1000	0.88	0.37	0	7.47E+06	8.60E+03	1.35E-02	303.3	-0.13	-0.158	6.6	313	313
1036	0.01	0.35	0	7.70E+06	8.65E+03	1.38E-02	308	-0.069	-0.096	6.6	313	313

QTOTAL= 185.38 J/CM*CM

ANNEXURE – B 1

EXTERNAL TPS DESIGN PHILOSOPHY

Thermal Environments

- ✓ Aerodynamic heating rates and total heat loads are computed for worst case trajectory considering 3-sigma dispersions in vehicle performance and atmospheric parameters.
- ✓ Heat load due to solar radiation and earth albedo is to be added to convective heating rates.
- ✓ Localized increase in heating rate in the vicinity of and on protuberance is to be considered.
- ✓ In the base region of the vehicle (of multi-strapon configuration) convective heating due to recirculating flow, radiation heating from solid particles in jet exhaust and radiation heating from hot nozzle divergent of liquid engines should be taken into account
- ✓ Effect of reflected radiation and recirculating flow after jet impingement on flame deflector at the time of lift-off.

Design practices being followed / recommended for external TPS design

For identification of thermal environments till PSLV program, worst case trajectory was being selected from among a set of actual control trajectories simulating winds, wind shear and gust at different key level altitudes along with 3-sigma dispersions in performance of various stage motors. For GSLV, ideal control trajectory along with 3-sigma dispersions in propulsion parameters and constant angle of attack of 4 deg throughout the ascent phase of flight was used. Considering the uncertainties in modeling of boundary layer transition, aerodynamic heating rates are computed assuming fully turbulent flow for ascent vehicles. Augmentation in heating rates in the vicinity of protuberances is based on **[23]**.

(a) Experimental data for similar protuberances available in literature

(b) Augmentation in heat transfer coefficient based on correlation formulae proposed by F. T. Hung involving pressure ratio before and after the shock formed ahead of protuberance

The dispersions in the atmospheric data (pressure, temperature and density are considered separately. The pressure distribution over the vehicle supplied is considered for heat load calculations. No perturbation over this is considered.

The computations of heat flux on spacecraft front surface after heat shield jettisoning is based on stagnation point heating computed for continuum flow and fully free molecular flow and use of bridging relation based on Knudsen number for transitional flow regime. A 15% margin on TPS thickness is considered to account for uncertainties in thermo-physical and optical properties of insulation material at elevated temperatures; perturbations in atmospheric density and temperature; inviscid flow field data variations. Details were accepted in GDRT (V & M) **[24, 25]**.

ANNEXURE – B 2

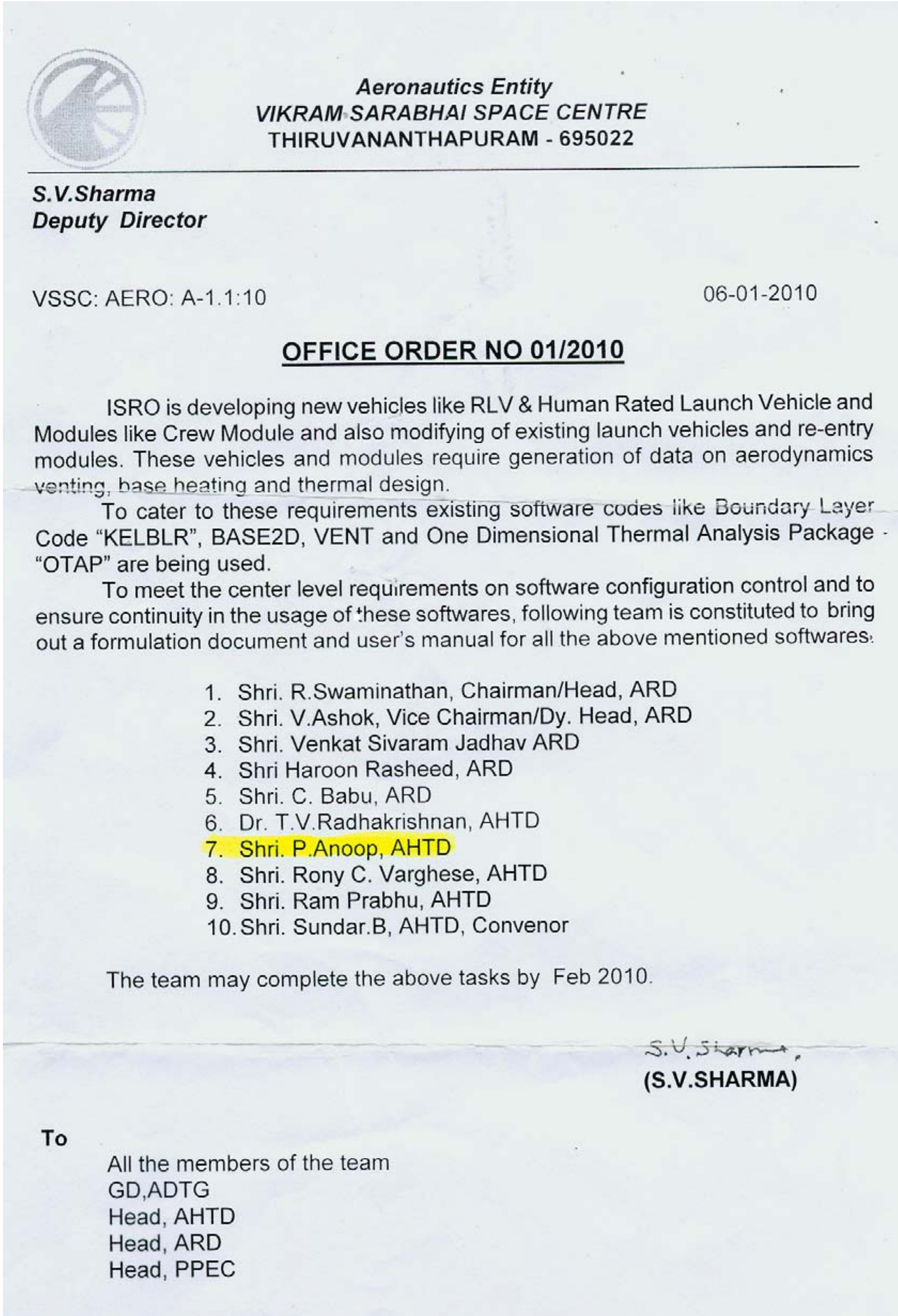

Aeronautics Entity
VIKRAM SARABHAI SPACE CENTRE
THIRUVANANTHAPURAM - 695022

S.V.Sharma
Deputy Director

VSSC: AERO: A-1.1:10 06-01-2010

OFFICE ORDER NO 01/2010

ISRO is developing new vehicles like RLV & Human Rated Launch Vehicle and Modules like Crew Module and also modifying of existing launch vehicles and re-entry modules. These vehicles and modules require generation of data on aerodynamics venting, base heating and thermal design.

To cater to these requirements existing software codes like Boundary Layer Code "KELBLR", BASE2D, VENT and One Dimensional Thermal Analysis Package "OTAP" are being used.

To meet the center level requirements on software configuration control and to ensure continuity in the usage of these softwares, following team is constituted to bring out a formulation document and user's manual for all the above mentioned softwares.

1. Shri. R.Swaminathan, Chairman/Head, ARD
2. Shri. V.Ashok, Vice Chairman/Dy. Head, ARD
3. Shri. Venkat Sivaram Jadhav ARD
4. Shri Haroon Rasheed, ARD
5. Shri. C. Babu, ARD
6. Dr. T.V.Radhakrishnan, AHTD
7. Shri. P.Anoop, AHTD
8. Shri. Rony C. Varghese, AHTD
9. Shri. Ram Prabhu, AHTD
10. Shri. Sundar.B, AHTD, Convenor

The team may complete the above tasks by Feb 2010.

S.V.Sharma
(S.V.SHARMA)

To

All the members of the team
GD,ADTG
Head, AHTD
Head, ARD
Head, PPEC